Solid State Lighting Program
Final Report

March 30, 2009

Novel Low Cost Organic Vapor Jet Printing of Striped High Efficiency Phosphorescent OLEDs for White Lighting

Work Performed Under Agreement
DE-FC26-04NT42273

Submitted by:

Universal Display Corporation
375 Phillips Blvd.
Ewing, NJ 08618

Principal Investigator:
Mike Hack, Ph. D.
(609) 671-0980 (ph.)
(609) 671-0995 (Fax)
mikehack@universaldisplay.com

Submitted To:

U.S. Department of Energy
National Energy Technology Laboratory
COR: Joel S. Chaddock
Joel.Chaddock@NETL.DOE.GOV

DISCLAIMER

Table of Contents

A. Table of Figures

B. Summary

In this program, Universal Display Corporation and University of Michigan proposed to integrate three innovative concepts to meet the DOE's Solid State Lighting (SSL) goals: 1) high-efficiency phosphorescent organic light emitting device (PHOLED™) technology, 2) a white lighting design that is based on a series of red, green and blue OLED stripes, and 3) the use of a novel cost-effective, high rate, mask-less deposition process called organic vapor jet printing (OVJP).

Our PHOLED technology offers up to four-times higher power efficiency than other OLED approaches for general lighting. We believe that one of the most promising approaches to maximizing the efficiency of OLED lighting sources is to produce stripes of the three primary colors at such a pitch (200 – 500 μm) that they appear as a uniform white light to an observer greater than 1meter (m) away from the illumination source. Earlier work from a SBIR Phase 1 entitled "White Illumination Sources Using Striped Phosphorescent OLEDs" suggests that stripe widths of less than 500μm appear uniform from a distance of 1m without the need for an external diffuser. In this program, we intend to combine continued advances in this PHOLED technology with the striped RGB lighting design to demonstrate a high-efficiency, white lighting source.

Using this background technology, the team has focused on developing and demonstrating the novel cost-effective OVJP process to fabricate these high-efficiency white PHOLED light sources. Because this groundbreaking OVJP process is a direct printing approach that enables the OLED stripes to be printed without a shadow mask, OVJP offers very high material utilization and high throughput without the costs and wastage associated with a shadow mask (i.e. the waste of material that deposits on the shadow mask itself). As a direct printing technique, OVJP also has the potential to offer ultra-high deposition rates (> 1,000 Angstroms/second) for any size or shaped features. As a result, we believe that this work will lead to the development of a cost-effective manufacturing solution to produce very-high efficiency OLEDs. By comparison to more common ink-jet printing (IJP), OVJP can also produce well-defined patterns without the need to pattern the substrate with ink wells or to dry/anneal the ink. In addition, the material set is not limited by viscosity and solvent solubility.

During the program we successfully demonstrated a 6" x 6" PHOLED lighting panel consisting of fine-featured red, green and blue (R-G-B) stripes (1mm width) using an OVJP deposition system that was designed, procured and installed into UDC's cleanroom as part of this program. This project will significantly accelerate the DOE's ability to meet its 2015 DOE SSL targets of 70 – 150 lumens/Watt and less than $10 per 1,000 lumens for high CRI lighting index (76-90). Coupled with a low cost manufacturing path through OVJP, we expect that this achievement will enable the DOE to achieve its 2015 performance goals by the year 2013, two years ahead of schedule.

As shown by the technical work performed under this program, we believe that OVJP is a very promising technology to produce low cost, high efficacy, color tunable light sources. While we have made significant progress to develop OVJP technology and build a pilot

line tool to study basic aspects of the technology and demonstrate a lighting panel prototype, further work needs to be performed before its full potential and commercial viability can be fully assessed.

C. Accomplishments

- **Built 2 generation OVJP research system at Princeton University capable of independently controlling the source temperatures.**

- **Demonstrated that the performance of device grown by OVJP deposition is similar to those grown by VTE deposition**

- **Modeled deposition flow dynamics from the nozzle**

- **Developed and demonstrated multi-nozzle printing**

- **Designed and procured a prototype OVJP deposition system**
  - (150 mm)2 substrate with (135 mm)2 print area
  - Six independently controlled sources
  - Modular nozzle head – multiple nozzles
  - Integrated with a dedicated vacuum thermal evaporation chamber, a load lock and a glove box (additional $280K)
  - System installed at UDC (June 2007)

- **Demonstrated RGB 6"x6" prototype lighting panel**
  - Red and Green emission layers were deposited by OVJP

- **Developed commercialization strategy**

D. Background

To date, the longest-lasting OLEDs have all been made by vacuum thermal evaporation (VTE). For this reason, small-molecule OLEDs dominate the commercial landscape for OLED displays. Color patterning is achieved by moving, in situ, a high-precision shadow mask during the deposition of RGB patterned pixels with a pitch of <100μm. Shadow masks are held under tension to counter thermal expansion and the pull of gravity, which becomes increasingly difficult with larger substrates. Though this manufacturing technology is being implemented today, the cost of this process may be a limitation in order to achieve the rigorous demands for both the display and lighting applications. For this reason, there is significant effort on developing alternative manufacturing processes and equipment platforms to achieve improved organic thin film deposition and pixel patterning.

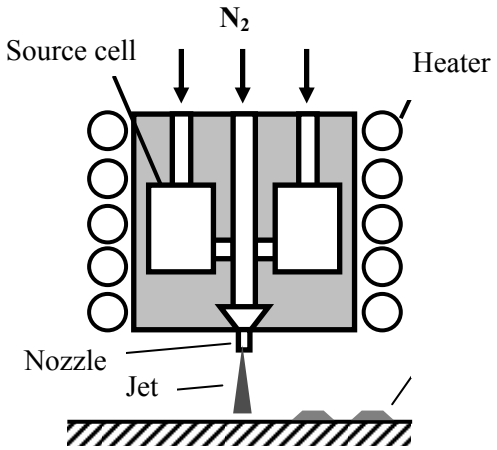

Figure 1: Schematic of the organic vapor jet printing (OVJP) apparatus, shown with two of the five source cells used in our experiments, a center dilution channel, and a modular collimating nozzle, all heated from the outside. A hot inert carrier gas enters the apparatus, picks up the organic vapor and ejects the gas mixture through the nozzle. The collimated vapor jet impinges onto a cooled substrate where the organic molecules selectively physisorb, forming a well-defined deposit.

One of these approaches, namely organic vapor phase deposition (OVPD) was pioneered by our team. Several years ago, the research team led by Professor Stephen R. Forrest at Princeton University demonstrated that OVPD could be used to deposit high-quality, organic films by using an inert carrier gas to precisely transfer organic materials onto a cooled substrate in a hot-walled, low-pressure (typically 10^{-3} – 1 Torr) chamber [2]. In OVPD, the organic, small-molecule materials are placed in external, separate, thermally-controlled cells. Once evaporated from their heated cells, the materials are entrained and transported by a pre-heated inert carrier gas, e.g. nitrogen, using gas flow rate, pressure and temperature as process control variables. The materials deposit down onto a cooled substrate within the hot-walled OVPD chamber from a showerhead located only several centimeters above. Because the deposition rate is primarily controlled by the flow of the carrier gas, deposition rates of 0.5-2 nm/sec, several times that for conventional VTE, can be achieved.

By comparison to VTE, OVPD may provide better film thickness control and uniformity over larger areas. With three-variable process control, OVPD offers more precise deposition rate and doping control at very low levels. As a result, sharper or graded layer interfaces may be more easily achieved by OVPD; multiple materials can also be co-deposited in one chamber without the cross-contamination commonly experienced in VTE.

Because the showerhead can be designed to maintain constant source-to-substrate distance over any size or configuration, OVPD may be easily scaleable for larger substrate sizes and shapes and also adaptable to roll-to-roll processing for flexible displays. In addition to enhanced device performance, the potential for materials' utilization of as much as 50% leading to lower raw material cost, less downtime and higher production throughput may provide key advantages over conventional VTE. One

potential limitation, however, is masked deposition as the mother glass size is extended above 1 meter. This was the focus of this program- namely to address the issues of high deposition rate, mask less deposition that is scaleable to large size panels to drive cost down to meet the SSL requirements.

OVJP is related to our previous high performance deposition technique OVPD for the low cost manufacture of OLEDs – see Figure 1. Prior to this program, OVJP had been applied to producing high performance organic TFTs (OTFTs), but has not yet been applied to phosphorescent doped heterojunction OLEDs. In addition, the dependence of printing speed on PHOLED device performance had not been characterized, and an in depth study of deposited film morphology and profile had not been pursued.

During this program the basic principles of OVJP as applied to multi-layer organic heterojunction organic light emitting devices were studied. Based on this work we developed and demonstrated OVJP printed striped PHOLED light source.

During first phase of the program we fabricated heterojunction PHOLEDs and optimize and characterize the individual Red, Green and Blue components, and correlate their performance to key OVJP deposition parameters. This work was completed on the research OVJP system operating at Princeton University. The Team then designed and built a second generation OVJP system that was installed at UDC. In the second phase we demonstrated a striped white light source.

E. Task 1.0 – Characterization and optimization of OVJP printed individual R, G and B stripes

Using the lab prototype organic vapor jet printing (OVJP) system small molecular weight, OLED materials were directly printed. Figure 2(a) schematically shows the apparatus and concept of OVJP. The proof-of-concept OVJP apparatus consists of a uniformly heated stainless steel cylindrical print head housing five separate source cells, a central dilution channel, a mixing chamber, and one or more outlet nozzles. Each cell can contain a separate molecular species, while the cell outlets connect via the mixing chamber. Three types of nozzles were used: One with a nominal inside diameter of 340 μm and a flow channel length of 2000 μm (Type I); an array of three 640 μm diameter by 800 μm long nozzles with a center-to-center spacing of 1410 μm (Type II-a), and 2100 μm (Type II-b); and an array of three 600 μm × 6000 μm slits with 800 μm thick wall and with a center-to-center spacing of 1410 μm (Type III). The substrates were mounted onto a water-cooled holder attached to a computer-controlled XYZ-positioning stage. The nozzle and the heated source cells remain stationary, while the substrate is translated continuously at a constant speed perpendicular to the jet direction in a path illustrated in Fig. 2(b). An inert carrier gas stream flows into a hot source container where it picks up the molecular organic species. The molecules enter a mixing chamber, and subsequently pass through a nozzle to form a highly directional jet.

It has been demonstrated that by varying the nozzle geometry OVJP can be used to print uniform $(1\ cm)^2$ flat organic films, as well as to deposit patterned organic structures. For example, a thin-film stack of 60nm thick NPD and 60nm thick Alq_3 was deposited

using a Type I nozzle. The nozzle-to-substrate distance was s =380 μm for depositing broad area flat films, and s=60 μm for depositing stripes. The substrate translation speed was 557 μm/s. Printing 30 10-mm-long lines with a center-to-center spacing of 320 μm resulted in a $(1\text{cm})^2$ thin film with a flat surface. These conditions correspond to a growth rate of 1.1 Å·cm^2/s. Using a Type II-a nozzle array resulted in a tripling of the growth rate, as expected. A scanning electron microscope (SEM) image (Fig. 2(c)) of the organic film stack cross-section exhibits a flat thin film deposit with a root-mean-square (RMS) roughness of 1.23nm, as determined using an atomic force microscope scanned across a $(20\ \mu\text{m})^2$ area.

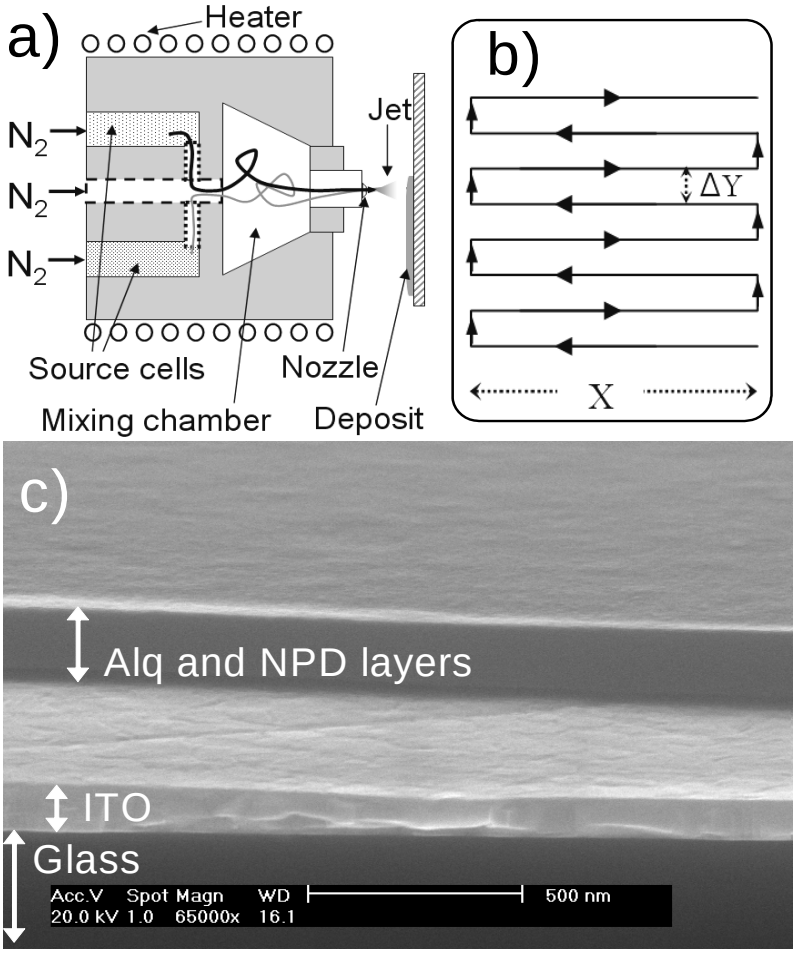

Figure 2. (a) Schematic of the organic vapor jet printing (OVJP) apparatus, shown with two of the five source cells used, a center dilution channel, and a modular collimating nozzle, all heated from the outside. A hot inert carrier gas enters the apparatus, picks up the organic vapor, and ejects the gas mixture through the nozzle. The collimated vapor jet impinges onto a cooled substrate where the organic molecules selectively physisorb.
(b) The translation path of the substrate in an X-Y plane perpendicular to the jet direction. Translation in X is at a constant speed, and the switching time from line to line in Y is < 0.6 s. *ΔY* denotes the spacing of lines which is adjustable.
(c) Scanning electron micrograph of a cross section of an organic thin-film stack printed on an ITO glass substrate using a 340 μm diameter nozzle, showing a nearly featureless flat surface.

By using a nozzle array, OVJP is able to simultaneously print multiple stripes of organic semiconductors. Figure 3(a) is an optical microscope image of one of three parallel stripes grown using a type II-b nozzle in a single pass, with other conditions similar to those used for the film in Fig. 1. Figure 3(b) shows the deposit thickness profile calculated from the optical interference intensity obtained under monochromatic light

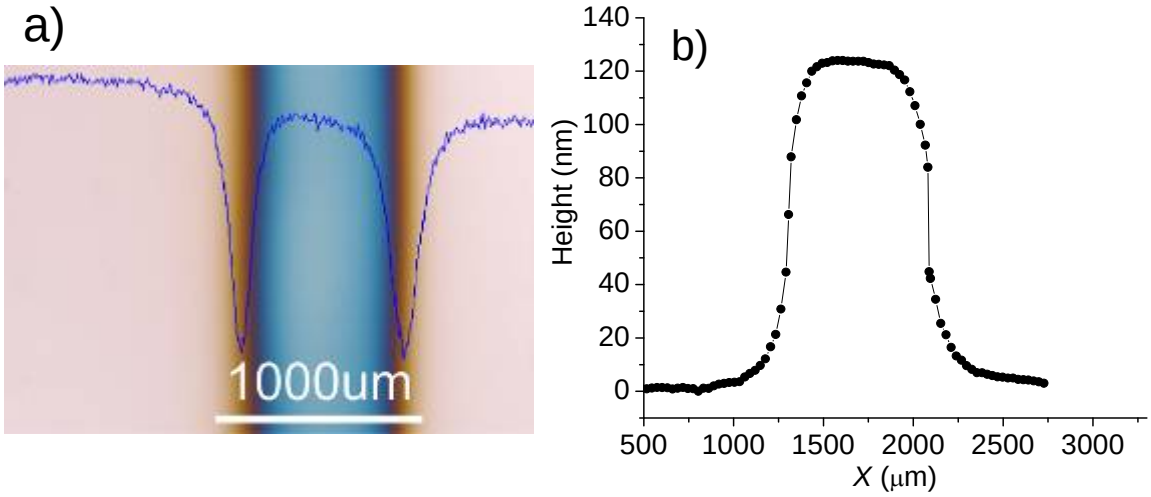

Figure 3: (a) Optical micrograph of one of the parallel Alq_3 stripes simultaneously printed on a Si substrate using a Type II-b nozzle array. The curve is a scan of the optical interference fringe intensity obtained for the stripe under 440 nm wavelength illumination. (b) Thickness profile of the stripe deposit in (a) calculated according to the optical interference intensity.

illumination at a wavelength of 440 nm. The three parallel organic stripes have thicknesses of (123 ± 8) nm, and full-widths at half-maxima of (780 ± 40) μm, compared with a nominal nozzle diameter of a = 640 μm. The approximate width of the usable, flat surface region of the stripe is approximately 680 μm.

These results show that high quality organic thin films can be deposited by OVJP at high speed.

F. Task 2.0 – PHOLED Device Characterization

The OVPD (organic vapor-phase deposition) and OVJP deposition technologies share many features such as material delivery system and heating controls, and so ideas proven out in the current (AIXTRON) OVPD system were used to design the pilot line OVJP machine built at UDC during Year 2 of this program. The system has been recently upgraded to provide for a more stable furnace temperature hence more stable deposition rates over a long time period. The source containers have also been slightly modified to provide higher deposition rates. The other goal was to improve the vacuum integrity

during heating up and cooling down cycles. Special care was taken to relieve mechanical stress due to thermal expansion and contraction.

We continued our efforts in establishing and optimizing the OVPD process using UDC's PHOLED material systems. In particular we have employed a green emissive dopant in a device structure with a 10nm thick hole-injection layer, a 30 nm thick NPD hole transport layer, a 30nm thick emissive layer consisting of CBP with the green dopant, a 5nm blocking layer , a 45nm thick Alq_3 electron transport layer and a LiF/Al cathode as shown in Figure 4. The doping concentration varied from 4.2 to 10.2 vol%. All organic thin films were deposited by OVPD.

Figure 5 shows the current-voltage-luminance characteristics of the OVPD-grown green PHOLEDs. At doping level of 8.2% luminous efficiency reaches 52.7 cd/A at 100 cd/m^2 and maintains 50 cd/A at a typical active matrix display luminance level of 1000 cd/m^2. The devices have been life-tested under the accelerated operational condition of $40mA/cm^2$, corresponding to an initial luminance L_0 >10,000 cd/m^2. The operational half-lives of these devices at these highly accelerated test conditions are found to be in the range of 150 to 170 hours. These results are comparable to that of similar devices fabricated by conventional technique of vacuum thermal evaporation (VTE).

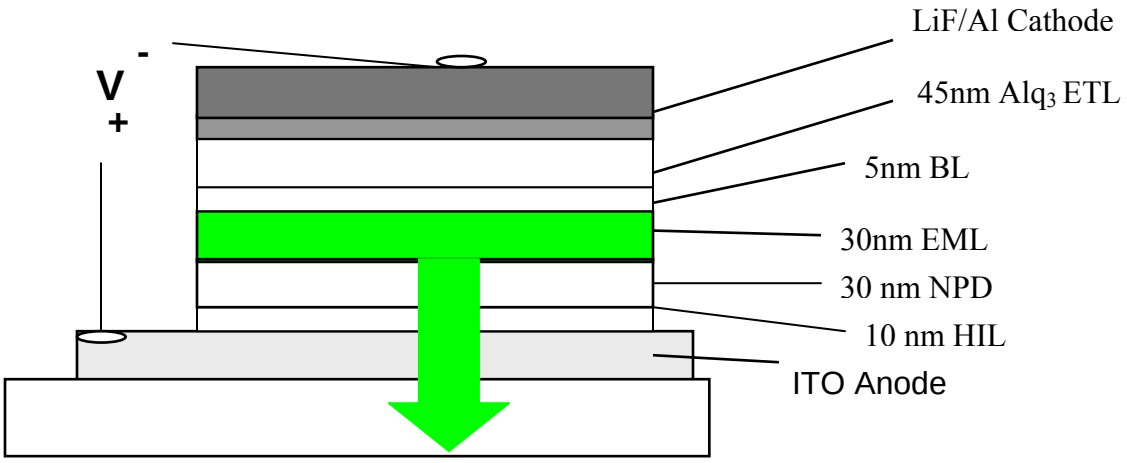

Figure 4. The green PHOLED layer structure consisting of ITO anode, 10nm thick hole-injection layer, 30 nm thick NPD, 30nm thick CBP/Green phosphorescent dopant, 5nm blocking-layer , 45nm thick Alq_3 and LiF/Al cathode.

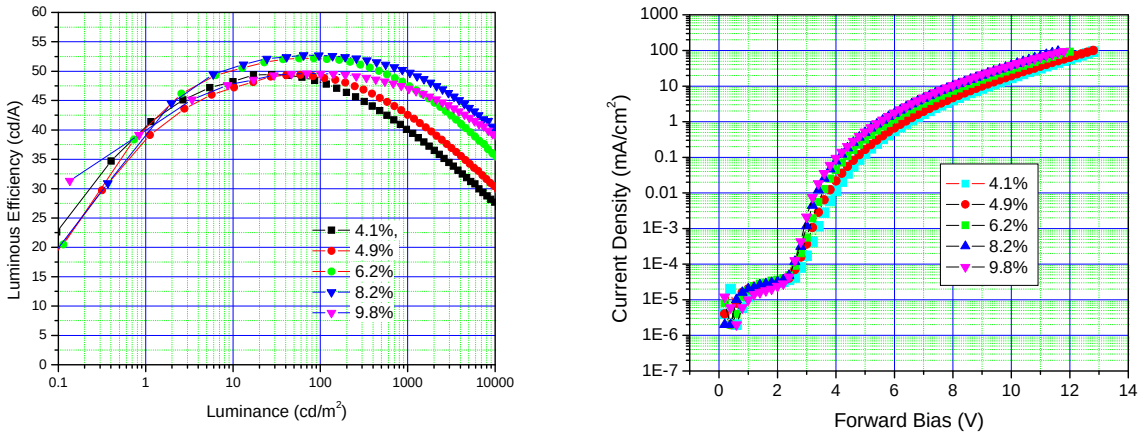

Figure 5. Luminous efficiency as a function of luminance of green PHOLEDs at various doping levels. At a typical display luminance of 1000 cd/m^2 the luminous efficiency reaches ~50 cd/A at a doping concentration of 8.2%.

G. Task 3.0 – OVJP Stripe Demonstration

While the Princeton proof of concept OVJP system can print individual materials, to accomplish the goals of fabricating multi-layer phosphorescent OLEDs to meet the target performance specifications, it was necessary to design a new custom Gen 2 OVJP system. The major improvement of the Gen 2 OVJP system over the proof-of-concept apparatus is its ability to independently control the source temperatures. This feature is required for fabricating the state of the art phosphorescent OLEDs such that the host and dopant printing rates can be independently controlled.

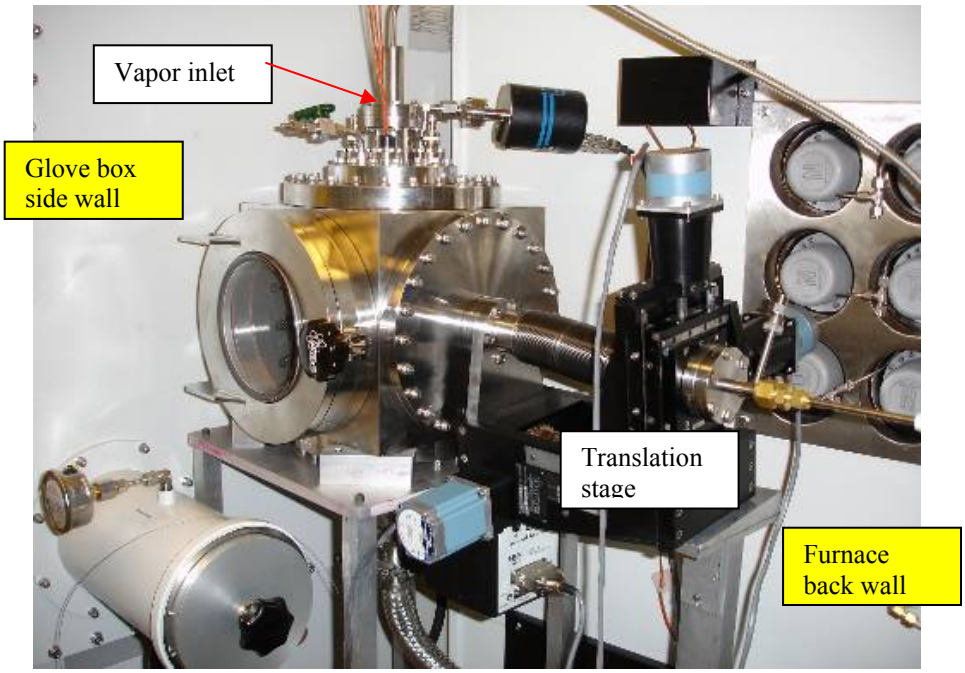

Figure 6: The OVJP vacuum chamber connected to the source furnace, the glove box and the XYZ translation stage.

For the Gen 2 OVJP system, the vacuum chamber is mounted to a glove box which in turn is connected to other VTE deposition equipment. As shown in Figure 6 the chamber has several thermocouple and electrical feedthroughs for the temperature monitoring and control and a mechanical feedthrough for the XYZ translation stage.

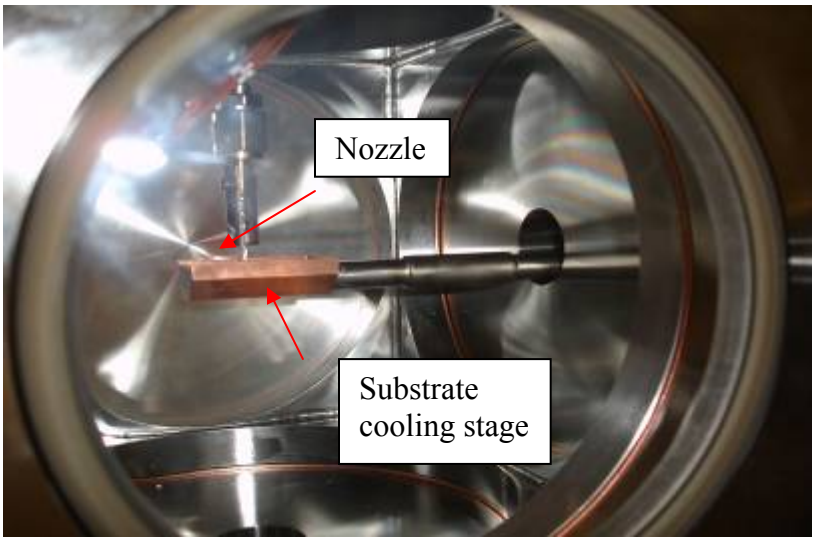

Figure 7: The vacuum chamber interior: the OVJP nozzle and the substrate cooling stage which is connected to the XYZ translation stage

Figure 7 shows OVJP nozzle above the water-cooled substrate holder which is mounted to the translation stage. The leading tube to the nozzle is connected to the sources housed in the furnace via a heated stainless line. The connected chamber and the source lines have also been pumped down successfully.

In the GEN 2 OVJP the organic vapor transported by ultra pure carrier gas such as N_2 or He is delivered via heated lines to a custom made glass nozzle to be printed onto the substrate. It is imperative that the transport line and the nozzle are heated sufficiently to prevent parasitic condensation. At the same time the line and the nozzle needs to be heated uniformly to prevent local overheating which may result in thermal degeneration of the material to be deposited. Several options of heating the nozzle were evaluated. Electrically insulated thin heating wires can be used to wrap around the nozzle tube but it is difficult to provide uniform heating at the very tip. Another approach was to enclose the nozzle and its leading tube in a heating jacket. In this method, only the very tip of the nozzle will be extended out of the outer tube to minimize heat dissipation. In each case, multiple thermocouples are mounted to the nozzle to control and monitor the temperature distribution. Test results showed that this approach can effectively heat up the nozzle tip by maintaining a constant temperature gradient between the outer tube and nozzle tube.

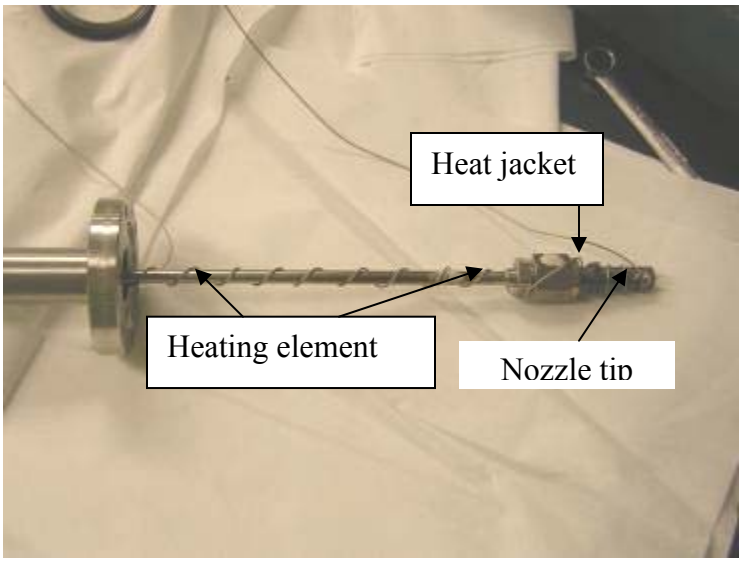

Figure 8: Glass nozzle and the gas inlet line enclosed in a heating jacket wrapped with an insulated heating element.

When the heating jacket is heated to 200ºC by a wrapped-on heating element (Figure 8) the temperature at the surface of the nozzle is only 5ºC lower. With proper installation of the heating coil, for example, embedded in grooves, the temperature control will be more effective and reproducible. This method allows also for heating of multiple nozzles by merely changing the shape of the jacket to fit and surround multiple closely spaced nozzles.

A phosphorescent OLED device consisting of printed doped emissive layer has been fabricated in the Gen 2 OVJP system. In order to print a continuous film the nozzle was programmed to travel back and forth in a pattern shown in Figure 9a. Figure 9b shows a Scanning Electron Micrograph (SEM) of a film surface printed with a 250μm nozzle traveling at approximately 2mm/s.

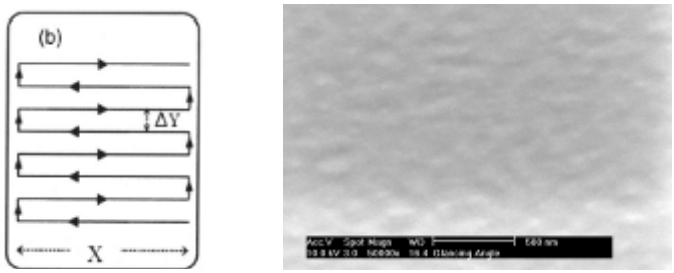

Figure 9: (a) the nozzle travel pattern for printing a flat film (b) SEM image of the printed surface

As shown in Figure 10a the PHOLED device is grown on an ITO coated glass substrate with a 400Å thick NPD hole transport layer by vacuum thermal evaporation (VTE), a OVJP printed 200Å thick 4,4'-bis(N-carbozolyl)biphenyl (CBP) with approximately 10% of *fac*-tris(2-phenylpyridine)iridium [$Ir(ppy)_3$] emissive layer and a VTE grown 200Å thick Alq_3 electron transport layer followed by a LiF/Al cathode layer. To accurately determine dopant concentration, the CBP deposition and $Ir(ppy)_3$ deposition rates were determined separately and then combined for co-deposition. A CBP source flow rate of 12 sccm, CBP source temperature of 290ºC, an $Ir(ppy)_3$ source flow rate of 3 sccm, and an $Ir(ppy)_3$ source temperature of 300ºC was used to deposit a 200A 10% doped emissive layer. A 35vsccm dilution flow was added and all downstream temperatures were set at 320ºC to ensure the elimination of all cold spots.

Several devices have been characterized using standard procedures including the electro-luminescence (EL) spectroscopy and current-voltage-luminance (J-V-L) characteristics. Figure 10b shows the EL spectrum characteristic of $Ir(ppy)_3$ emission with the peak emission wavelength at 511 nm,. From I-V curves shown in Figure 10c we find that voltage for a forward current density of $10mA/cm^2$ is about 9-10V. Device 1A and 1B lie on the same substrate while Device 2A is from a separate OVJP deposition.

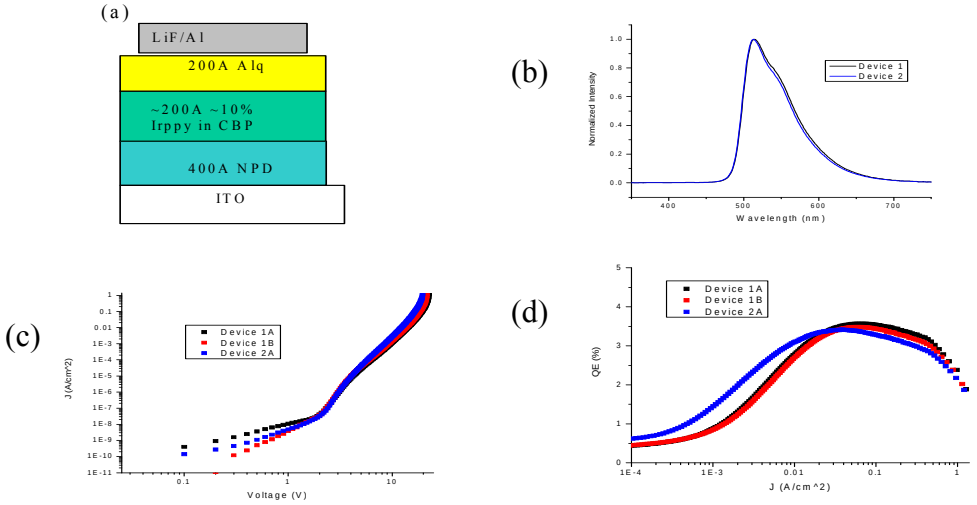

Figure 10: a) The device structure with a 200Å doped emissive layer printed by OVJP, (b) the EL spectrum, (c) the I-V characteristics and (d) the external quantum efficiency of the PHOLED

Figure 10d shows the external quantum efficiency (EQE) as a function of current density. A maximum EQE of 3.6% is reached at about 60mA/cm^2. At this point it is important to note that the efficiencies of the OVJP deposited phosphorescent OLED are not equal to the highest reported efficiency Ir(ppy)$_3$/CBP devices due to the absence of the exciton blocking layer (EBL). It can be reasonably assumed that once this layer is introduced into the device structure, the quantum efficiency will dramatically increase to approximately 8%. Reported structures without EBL's grown in VTE have shown quantum efficiencies around 0.2% proving the OVJP device highly competitive.

Using the recipes that have been developed to reliably produce single color arrays using the OVJP process were combined to produce tri-color OLED arrays. The red and green OLEDs are made using UDC RD-15 and Ir(ppy)$_3$ phosphorescent emitters doped into a 300Å CBP host layer. The blue phosphorescent OLEDs are produced with a neat film of 250Å FIR6 preceded by a 150Å mCP electron blocking layer. Figure 11 shows a tri-color array of OLED stripes made by depositing the emissive layers using the OVJP with and without a diffuser. Once the diffuser in placed in front of the stripes, the image appears white.

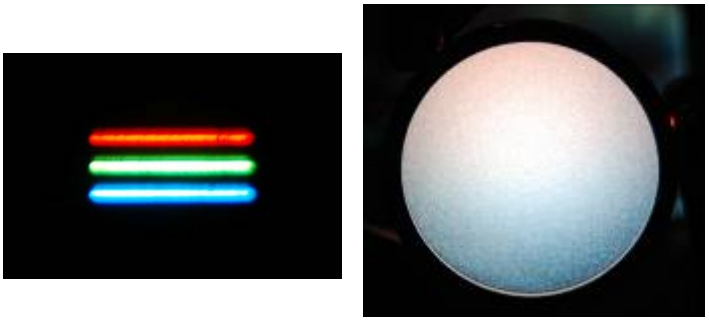

Figure 11: Tri-color array using OVJP deposited emissive layer with and without diffuser

As the performance of the OVJP deposited materials continued to be optimized, comparisons to the same materials deposited by VTE were made. Although the performance of OVJP deposited materials had improved, the performance is still less with higher turn on voltages and lower efficiencies. See Figure 12.

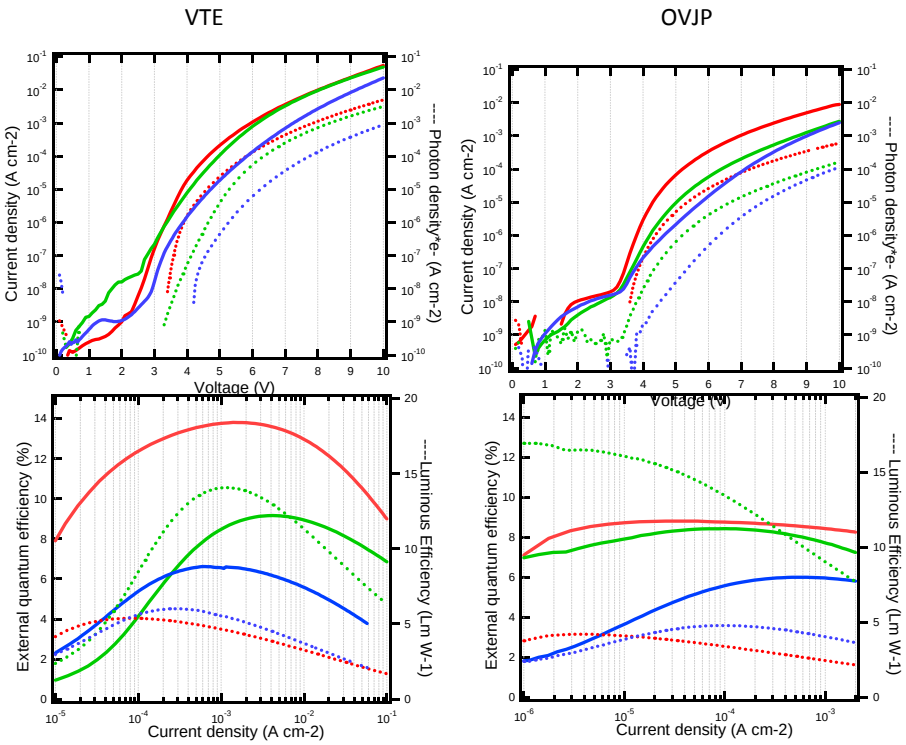

Figure 12: Performance comparison of devices deposited by VTE and OVJP

One of the largest problems with previous devices made by depositing the emissive layer by OVJP has been a high turn on voltage of both the red and green segments. The turn on voltage has been varying, sometimes being very high and other times it was comparable to devices deposited by VTE. One deposition parameter that has been investigated is the substrate temperature during OVJP deposition. It was thought that the substrate temperature could be influencing the efficiency of the devices. Green OLED devices with the emissive layer deposited by OVJP were grown with varying substrate temperature from -10C to 50C. It was found that by increasing the substrate temperature from -10 to 50C the peak luminous efficiency doubled, from 6 to 12 lm/W. See Figure 13.

Substrate temperature:

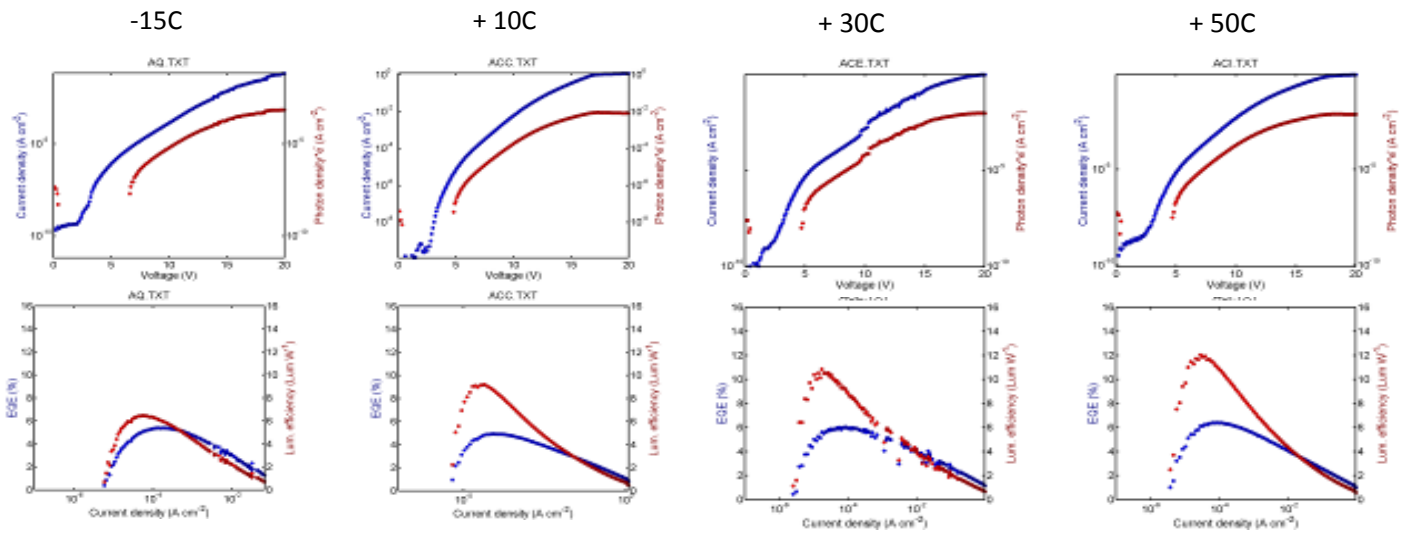

Figure 13: Efficiency of green $Ir(ppy)_3$ phosphorescent emitters doped into a 300Å CBP host layer deposited by OVJP at different substrate temperatures.

By using the substrate temperature data and continuing to optimize the device structure, the performance of the red and green devices has improved resulting in efficiencies similar to those that have been achieved by VTE. Although the temperature did have a big influence in the red and green devices, there was no temperature influence on the blue device. The performance data is summarized in Figure 14 below along with the data for two different white devices that were the result of the segmented colors.

Color	Process	ηEQE [%]	ηp [lm/W]
Red	OVJP	9.4±0.5	4.7±0.5
Red	VTE	12.6±0.1	4.9±0.1
Green	OVJP	8.6±0.7	16.5±1.2
Green	VTE	8.9±0.3	13.3±0.5
Blue	OVJP	5.4±0.6	4.2±0.5
Blue	VTE	6.0±0.9	5.5±0.9
White 1 (0.33, 0.33)	OVJP	7.0±0.3	4.9±0.2
White 2 (0.40, 0.31)	OVJP	7.1±0.3	7.0±0.4

Figure 14: Summarized performance comparison of materials deposited by VTE and OVJP

H. Task 4.0 – Demonstration of OVJP Parallel Printing

To enable high manufacturing throughput, it is expected that multiple OVJP nozzles will be utilized to simultaneously print parallel OLED lines. It is therefore essential to understand the flow patterns associated with multiple closely spaced nozzles. As seen in Figure 12 simulations of flow patterns have been performed to model the velocity profile of the carrier gas exiting multiple nozzles. Figure 15a shows the velocity profile in the presence of only one 20 μm nozzle. However, when we introduce three 20μm nozzles 50 μm space apart there is significant guarding of the flow as shown in Figure 15b. The velocity of the flow exiting the center nozzle has a much smaller component parallel to the substrate. This would result in less spreading of the deposition upon exit from the nozzle, likely leading to better resolution.

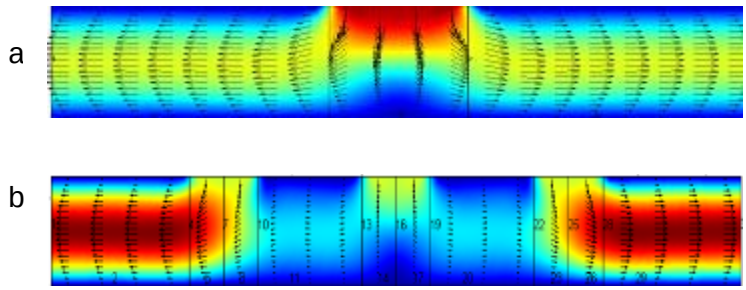

Figure 15: FEMLab simulations of carrier gas flow out of nozzle. (a) one 20μm nozzle, (b) three 20μm nozzles spaced 50μm apart.

The performance and reliability of an OVJP system can be improved by reducing the surface area of tubing brought into contact with organic vapor. Organic vapor appears to interact with metal, even if the metal is hotter than the organic material's vaporization temperature. This interaction contributes to a several minute delay between the start of organic vapor flow and the start of printing. A greatly simplified vapor generator for the OVJP system can be based on the same design used to perform organic vapor phase deposition (OVPD) experiments. This design is capable of controlled co-deposition and it has proven extremely reliable.

Multiple nozzles provide a clear path to further scale-up of OVJP for large area patterning applications. In order to produce uniform deposition in a large array, nozzles will have to be combined with vacuum draws to provide an escape route for spent carrier gas. In addition to increasing the number of nozzles, nozzle size may be needed to be made smaller in order to improve the resolution of printed devices.

Possible configurations for parallel nozzle arrays were modeled using the Direct Simulation Monte Carlo (DSMC) method developed by Bird.[i] The combination of a highly confined space, low pressure, and large velocity and temperature gradients present in an OVJP nozzle necessitates the use of a DSMC model. This model was implemented using MONACO code written by the research group of Prof. Boyd at the University of Michigan.

Several variations on the cross stream design for individual nozzle elements of an array (Figure 16) were evaluated. It was found that the presence of an enclosure over the nozzles tended to produce a shunted flow between the nozzle and outlet. The enclosure modeled allows pressure to build up between the nozzle and substrate, and the shunted flow may allow organic material to escape, both reducing deposition efficiency. While the use of an enclosure to guide vapor flow should not be ruled out prematurely, early modeling suggests that more open designs are preferable.

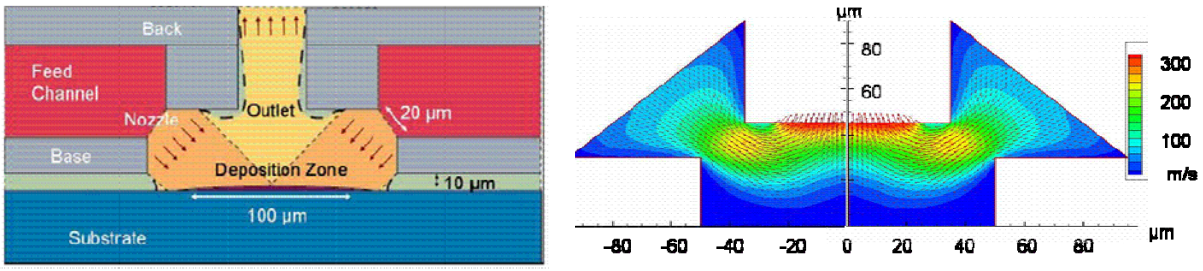

Fig. 16 (right) Cross section of proposed nozzle unit for multiple nozzle array. The enclosure around the deposition zone was intended to direct the jet and increase uniformity of deposition. (left) Simulations indicate that carrier gas flow is shunted between nozzle and outlet in this configuration. A large fraction of organic material may exit through the nozzle as well. Simulation parameters are 38 Torr and 600 °K in feed channel and 380 mTorr at the outlet.

Previous work in Organic Vapor Deposition and Physical Vapor Deposition suggests that reducing background pressure in the deposition zone improves deposition efficiency.[ii, iii] Modeling studies of OVJP have also suggested that a decrease in background pressure can increase resolution as well.[3] With this in mind, a simple nozzle array which provides an unobstructed path for carrier gas to exit the deposition region is shown in Figure 17. This nozzle array is easy to fabricate and will minimize pressure in the deposition region.

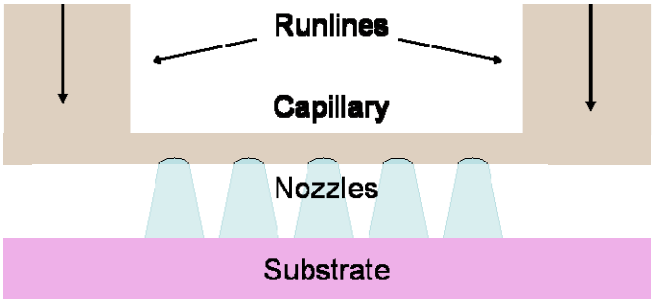

Fig. 17 (right) Diagram of simplified nozzle array. Steel capillary connecting two feed lines is drilled with nozzles of 10 to 100 µm diameter. Lines are drawn by translating the substrate underneath the nozzle array.

Producing organic vapor efficiently and delivering it through a nozzle creates a competing set of requirements for OVJP operating pressure. Evaporation rates proceeds most efficiently at low pressure, since background gas tends to impede the motion of evaporated particles from their source at higher pressures. High carrier gas pressure can also produce an overly dilute vapor mixture.

While operating at lower pressure facilitates evaporation, it could complicate vapor delivery by nozzle. Maintaining mass flow rate per unit nozzle cross section requires a driving pressure that scales as $O(L^{-1/2}/D)$ where L is nozzle length and D is the nozzle diameter. Smaller nozzles require more driving pressure. Even higher pressure may be required to supply a complex print head with many nozzles connected by channels.

Placing a pump between the sources and nozzle would reduce the tradeoff between vapor production at low pressure and jet formation at high pressure. A pump can draw vapor generated in the backline at low pressure and compress it to drive a nozzle flow. A pump will also provide flow control, allowing the flow of organic vapor to be rapidly attenuated. The ability to pulse flow would enable rapid printing of complex structures, since vapor flow could be started and stopped as a pattern requires.

Compression is expected to allow faster vapor generation, smaller feature size, and more control over printing. These benefits, however, do not come without potential complications. A compressor would concentrate organic vapor as it increases overall pressure. Partial pressure of organic vapor may exceed its equilibrium vapor pressure in some cases. Transport of supersaturated vapors and their use to grow electronic films will need to be studied to establish the feasibility of a compression system.

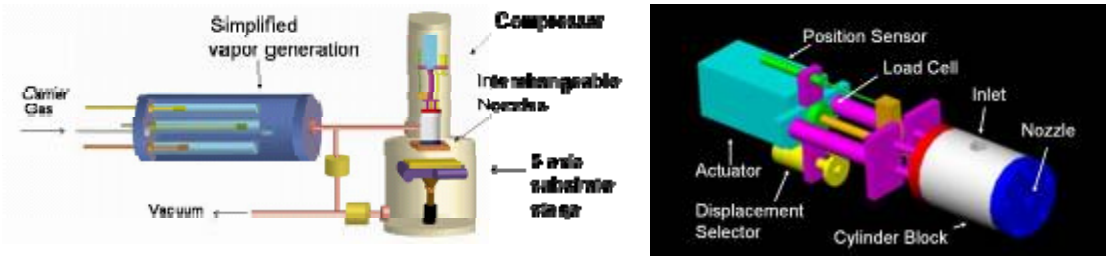

Figure 18: (left) Conceptual drawing of improved OVJP system. (right) Rendering OVJP compressor pump.

Since undesired condensation of vapor would be a problem with any compression system, it should be resolved to a relatively simple platform before proceeding to design more complex pumping solutions. To this end, a pneumatically actuated 3 cc piston pump is currently being fabricated. See Figure 18 a conceptual drawing of the OVJP system with the compression system.

With compression and specialized nozzles, it may be possible to generate vapor jets with velocities well in excess of the speed of sound using OVJP. Highly ordered pentacene films have been grown using a supersonic molecular beam. Incident molecules in a supersonic beam hit a substrate with higher than thermal energies. Highly

energetic molecules are able to widely sample a cold surface to find resting places that minimize energy. High energy beams were found to produce fewer islands, suggesting that molecules can diffuse greater distances to incorporate into islands.

The actuator assembly for a high temperature dry pump for the compression of organic vapor has been completed. The pump is now ready to test and is shown in Figure 19. It has a stroke time of ~100 ms, allowing a cyclic rate of several Hertz. The pump is designed to operate best at temperatures above 200°C and feed pressures of ~5 Torr, so testing will require vacuum. A small thermopile on a movable stage will be used during testing to characterize the jet of hot vapor produced by the pump. Although the pump was completed, it was not tested due to chamber restrictions and the development of the new multi-nozzle array.

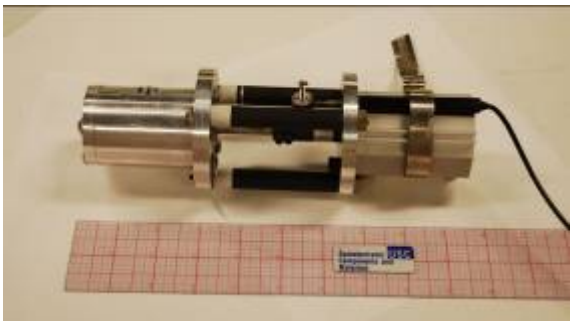

Figure 19: A high temperature dry pump designed to compress organic vapors for delivery to nozzles.

I. Task 5.0 – Design, procurement and installation of OVJP equipment at UDC

To produce the final hardware deliverable of prototype lighting panels with RGB PHOLED stripes printed by OVJP an OVJP system capable of printing over a 6" x 6" substrate was designed, procured and installed at UDC. It was decided that the system built needed to be a stand-alone OVJP system rather than attaching the OVJP with an existing UDC deposition tool. In this system the PHOLED emissive layers will be deposited and self-patterned by OVJP, while the non-patterned organic films such as the electron and hole transport layers will be deposited in an integrated vacuum thermal evaporation (VTE) chamber. Although this approach will result in additional expenditures of approximately $300K over and above the funds outlined in the original proposal, a standalone system presents significant advantages including a higher throughput, more versatility in the range of device structures that can be grown, and the ability to directly compare devices grown by OVJP with those by conventional VTE, of which UDC has a wealth of data on device efficiency and reliability.

The OVJP module of the system is designed to have the following features:

1. Six individually controlled sources, external to the deposition chamber, enabling the deposition of at least three emissive materials doped in three different host materials sufficient for a full color combination.
2. Each source cell will be heated in an individual furnace and the vapor delivery is regulated by a mass flow controller and three valves: the inlet, outlet and the bypass. This configuration minimizes the back diffusion of source material and cross-contamination between different sources.
3. A single print head will be employed to print the red, green and blue stripes sequentially so that the vapor delivery lines can be relatively simple. The print head can contain either a single or multiple nozzles.
4. The substrate will be mounted on a water cooled stage which in turn is moved by an XYZ translational control to create the printing patterns. The range of translation is 150mm in the XY dimensions and 50mm in the Z dimension. The accuracy of the XYZ control will be ± 20 μm.
5. The deposition chamber will be pumped by a dry mechanic pump to reach a 50-mTorr base pressure with a helium leak rate < 10^{-8} mBar-liter/sec.

Some of these features are illustrated in the following figures. Figure 20 is a three-dimensional conceptual design of the OVJP module showing a vacuum deposition chamber and six source ovens arranged in two stacks. Organic vapor transported by nitrogen carrier gas exiting from each oven will combine into a single line which enters the deposition chamber from the top. Inside the chamber the line ends with a print nozzle head described in the previous report. Figure 21 shows more details of an oven back wall onto which three high-temperature valves are mounted. Figure 22 shows a source oven with top and bottom heating plates. There will be additional heaters in each oven, especially at the vapor outlet valves to minimize the heat sink effect of the valve actuators and to maintain the uniformity and stability of the oven temperature. One prototype oven will be built first to test the temperature uniformity and stability to provide further guidance to the final design. Thermocouples will be distributed throughout the vapor transport line to monitor and control the temperature profile to prevent local cold spots where parasitic condensation may occur or hot spots which may affect the material quality. For the same reason it is critical to properly insulate the external vapor lines although for simplicity the insulation is not shown in the figures.

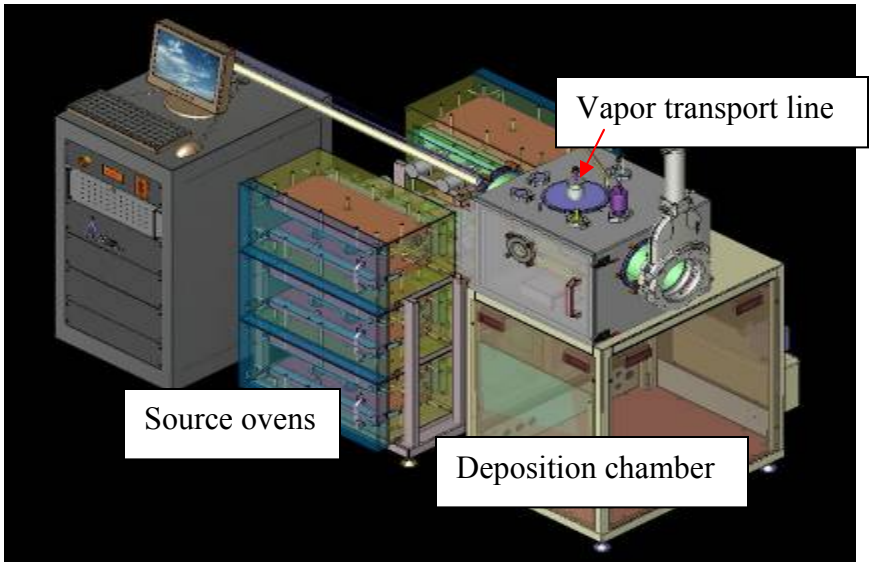

Figure 20: The OVJP module with six source ovens. Thermal insulation pm the vapor line is not shown.

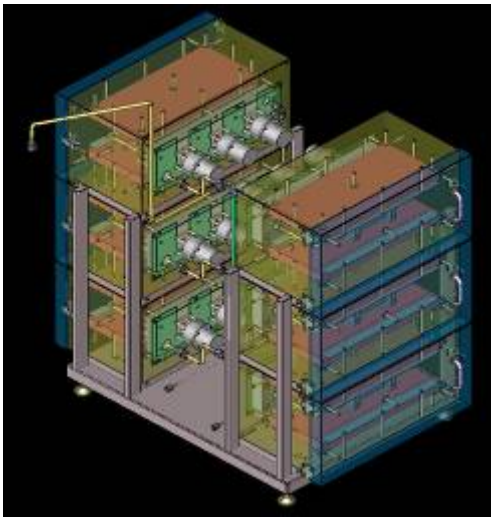

Figure 21: Six source ovens in two vertical stacks, mounted on a frame.

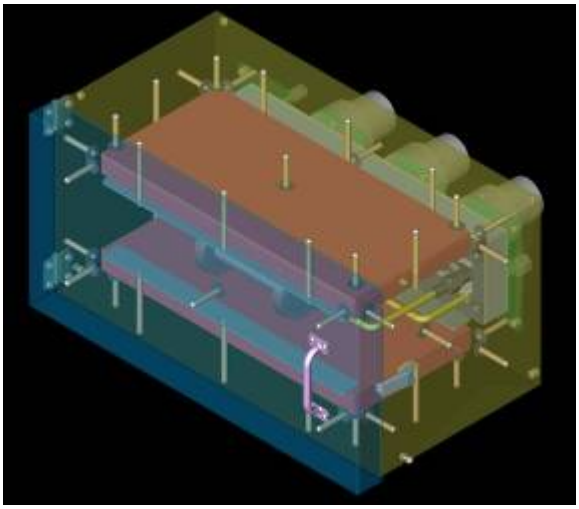

Figure 22: Schematic drawing of a source oven containing a source cell (partially concealed) and actuators of the three hot valves.

Figure 23 shows a layout of the stand-alone prototype OVJP system. In the center is a load-lock which also serves as a substrate flipping stage as well as the substrate and shadow mask storage. (The substrate is facing down for the vacuum thermal evaporation is facing up for OVJP.) Although OVJP is a mask-less operation, shadow mask is needed for the deposition of the electrode layer. A substrate can be loaded in the glove box or directly into the load lock and unloaded into the glove box for encapsulation.

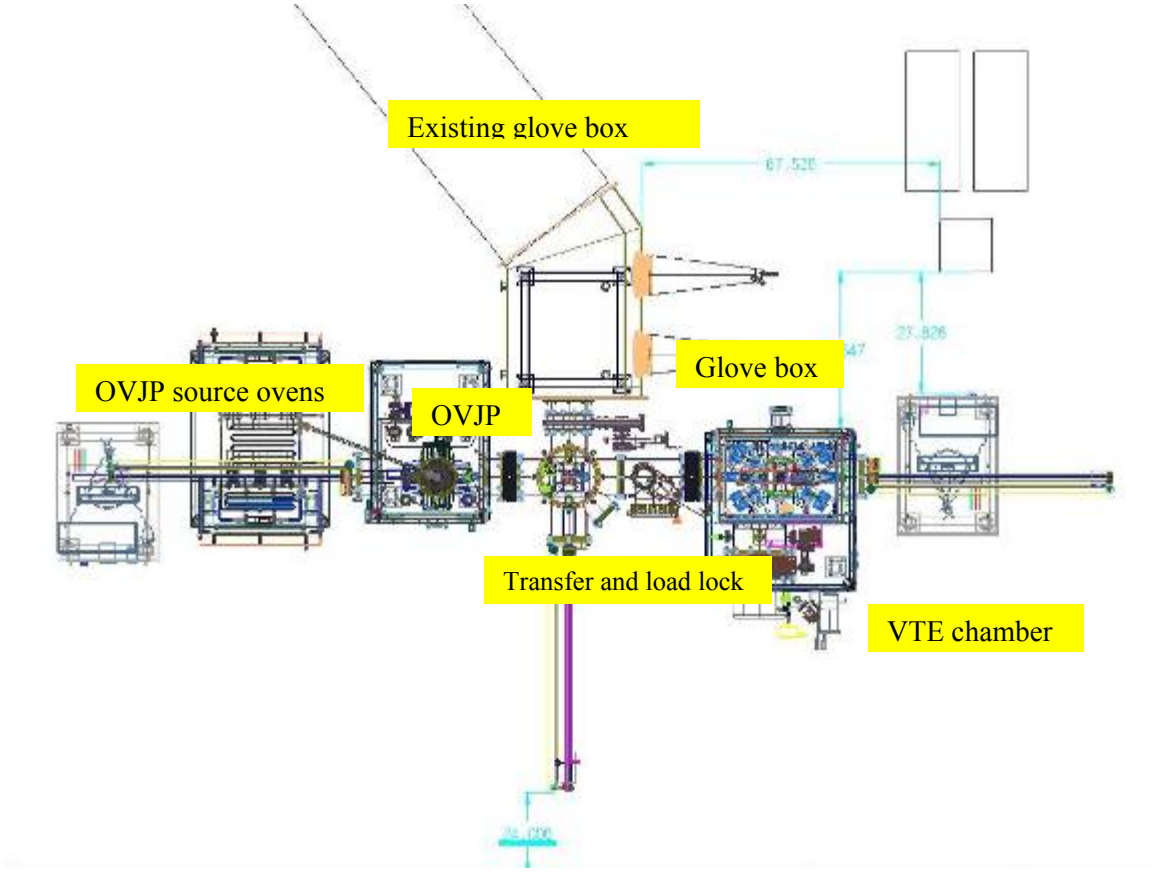

Figure 23: Floor plan of the UDC OVJP system consisting of an OVJP chamber, OVJP source ovens, a vacuum thermal deposition chamber and a loadlock-sample transfer chamber, connected to a glove box.

The VTE module includes the VTE chamber and a load-lock-transfer chamber that connects the OVJP to the VTE modules and interfaces with the glove box. Figure 24 shows a 3-D drawing of the VTE and transfer chambers, and the glove box. While the OVJP can perform self-patterning, shadow masking is required for the VTE. Three pieces of substrate and shadow masks can be stored in the transfer chamber where they can be coupled or separated. The substrate can be flipped in the transfer chamber according to the direction of deposition (face-down for VTE and face-up for OVJP).

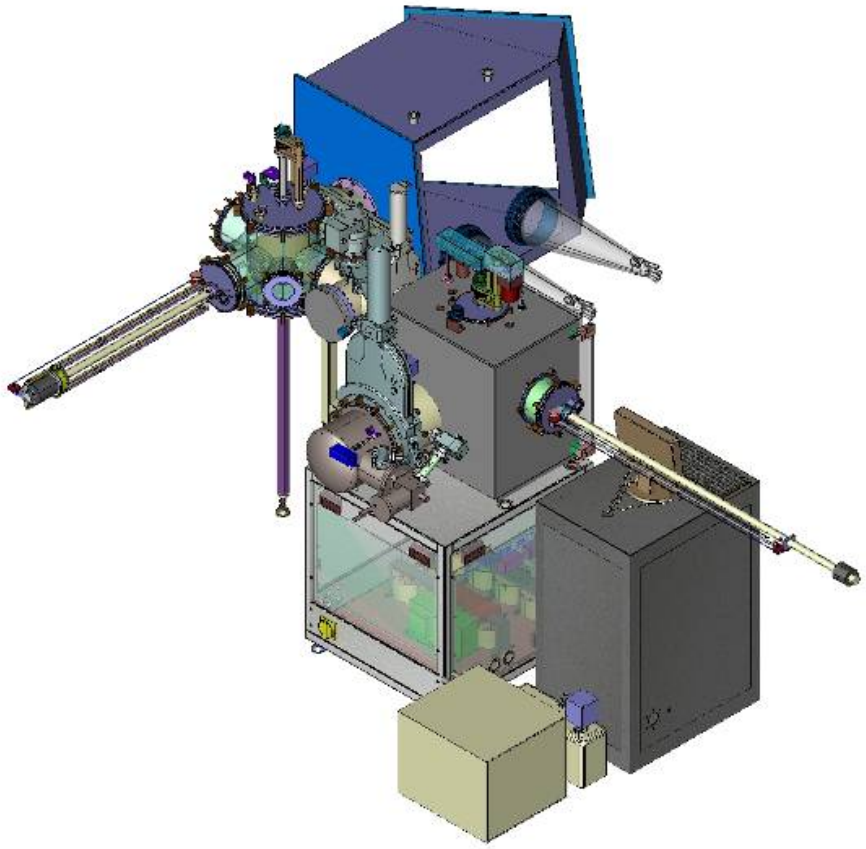

Figure 24: The vacuum evaporation chamber and the transfer/load-lock chamber connected to a glove box and to the OVJP chamber (not shown).

While the VTE technology is well established and a VTE chamber with multiple organic sources is considered standard equipment, it is common to deposit the metals in a separate chamber. In our tool we have decided to perform both these functions in a single chamber, so special care was taken in the design of this module to avoid cross contamination problems. Figure 25 shows the bottom plate of the VTE chamber with a total of ten evaporation sources: seven for the organics, three for the cathode materials. Proper shielding is provided between sources to prevent cross contamination and in particular, high temperature metal sources are not adjacent to any of the organic sources. Five crystal thickness monitors will be installed enabling simultaneous depositions of host and dopant materials, a technique essential to making high efficiency phosphorescent OLEDs.

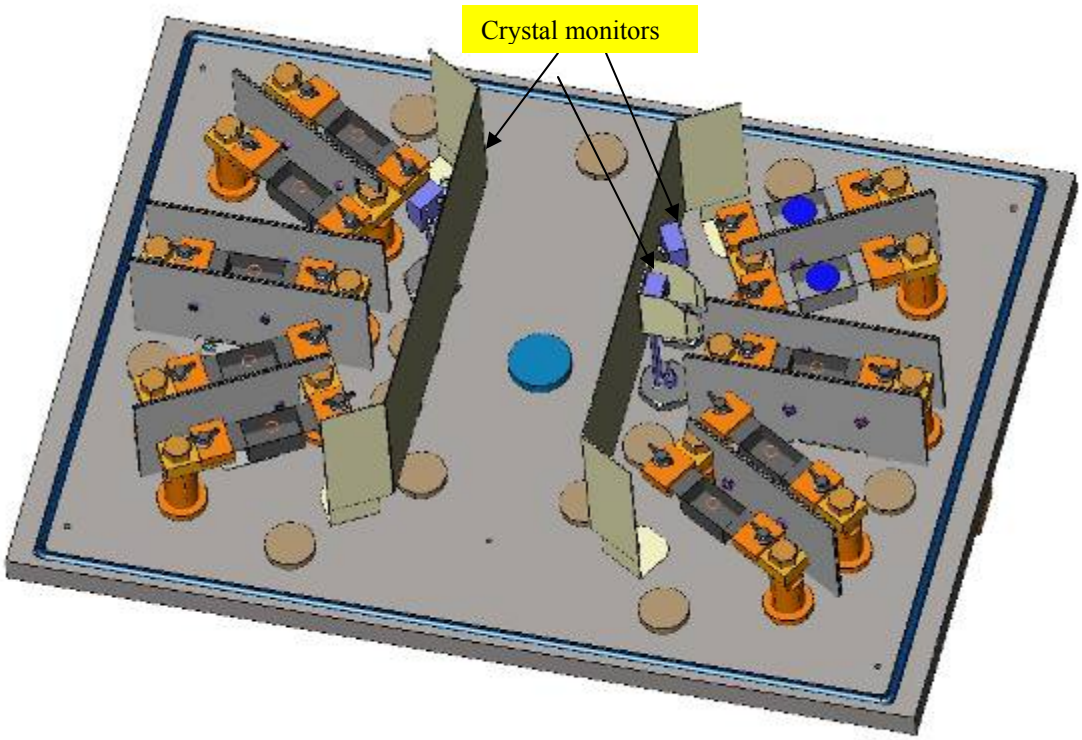

Figure 25: Base plate and the layout of the evaporation sources in the VTE chamber. Three crystal thickness monitors shown are for the low rate, i.e., dopant depositions, two other thickness monitors are mounted near the substrate (not shown).

During the assembly and testing of the OVJP system, there was a major issue with the hot valves that control the gases for the sources in the OVJP. The valves as delivered were found to be leaking at room temperature. They were returned to the manufacturer multiple times before the manufacturer determined the cause of the defect. The defective valves were all been replaced, tested and reinstalled on the tool. This issue delayed the project by approximately 2 months.

Once the new OVJP system was fully assembled and completely insulated, thermal testing started. An issue with vacuum tubing fittings mounted inside the oven leaking while the oven was hot. The fitting problem was a combination of a wrong type of fitting that would damage the sealing seat when tightened due to the torque that was applied, and the wrong type of seal gasket. Angstrom Engineering installed a new type of fitting and switched from a stainless steel gasket to a silver coated nickel gasket. The silver coated nickel gasket creates a better seal since the nickel is soft and conforms to both

seats when tightened. All the fittings were replaced and the ovens have been temperature cycled to 300ºC multiple times with no leaks.

In April 2007, the initial acceptance test was completed at Angstrom Engineering. During the testing, several materials were successfully deposited using the OVJP system and are shown in Figure 26. Both red (RD07) and green ($Ir(ppy)_3$) dopants and host (CBP) materials were deposited along with single films of CBP and Alq.

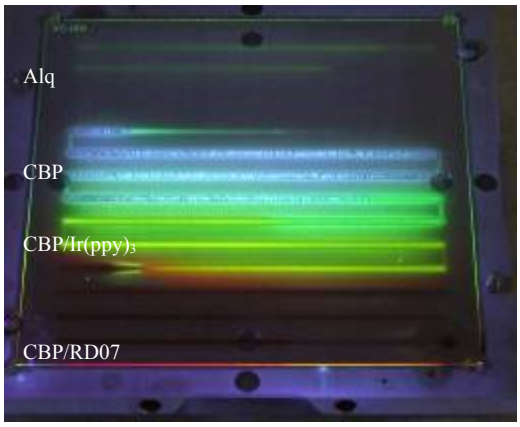

Figure 26: Photoluminescence of materials that were deposited by the Angstrom OVJP during acceptance testing.

Although materials were successfully deposited, bowing of the glass substrate was observed during some of the depositions. It is believed that the bowing is caused by non-uniform heating of the substrate from the close proximity of the hot nozzle to the glass substrate. The surface temperature of the substrate was measured by attaching temperature tapes to the center of the glass substrate and moving the nozzle at a height of 1mm above the stickers at a rate of 1mm/sec with no gas flow. The maximum temperature triggered on the tapes was 149C. Several equipment modifications were completed to reduce this temperature, which includes; polishing the substrate holder for better thermal conduction; reducing the nozzle outside diameter, thus reducing the thermal mass that is close to the substrate; installing a heat shield that that surrounds the nozzle to reduce the radiation of heat.

Angstrom Engineering also installed upgrades to the OVJP system which include changing the mass flow controllers from a maximum of 100 sccm to 50 sccm, relocation of furnace monitoring thermocouples from gas feed tubing to the source and installing a bypass valve and line in the carrier gas line just before the line enters the chamber. The mass flow controller repeatability is 1% of the full range of the mass flow controller. Since most of the testing to date has been with flows ranging from 3 to 20 sccm, the controller range needed to be reduced for process repeatability. From our experience with the Aixtron OVPD system, we have found that it takes much longer for the source temperature to reach the set point than the oven. By moving the thermocouple to the source, the source temperature will be monitored to ensure that it is at the set point prior to the start of processing. The bypass valve and line will connect the carrier gas line just before the chamber to the vacuum pump. This will be installed to reduce the deposition delay and allow for flushing the lines to remove contamination.

The system was tested with the new upgrades. The deposition delay time from when the source valve was open to when the material was being deposited through the nozzle has been reduced. This was done by opening the bypass valve prior to opening the source valve, eliminating the flow restriction of the nozzle and allowing the material to move quickly through the tubing to just above the chamber, then closing the bypass valve after a short period of time to force the material through the nozzle. Further testing will be required to determine the optimum timing for opening and closing the bypass valve to achieve the required deposition parameters.

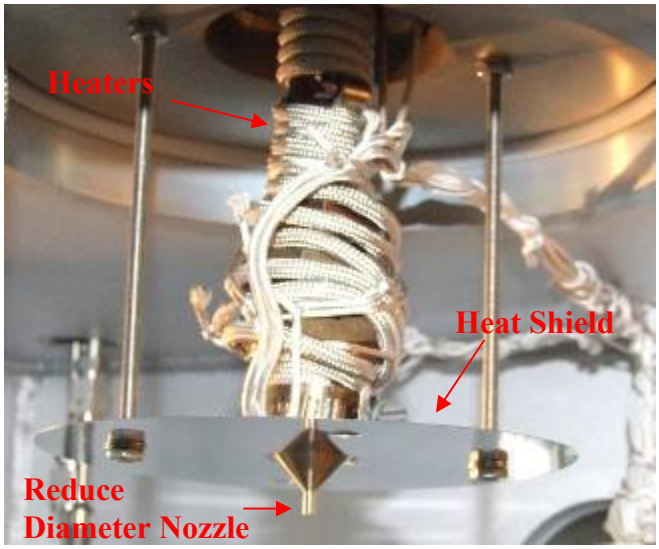

Figure 27: Picture of the reduced diameter nozzle and the newly installed heat shield.

The system with the new heat shield and nozzle was tested for substrate bowing. See Figure 27. The system was set at process conditions which substrate bowing was observed during the acceptance testing in April with no bowing observed. The process conditions were then changed to condition which would transfer more heat to the substrate; reducing the tip height to the substrate from 1mm to 0.5 mm, reducing the substrate write speed from 1mm/sec to 0.5mm/sec and doubling the flow of hot gas through the nozzle. No substrate bowing was observed.

The system was disassembled and crated, and was shipped to UDC in June 2007.

The Angstrom OVJP system was completely reassembled in the UDC cleanroom and all the facilites were connected in July 2007. See Figure 28. The system was turned on and tested by depositting stripes of doped and undoped material. These stripes were uncalibrated and used only for testing to ensure that the source heaters and mass flow controllers were operational.

Figure 28: OVJP System in UDC's Cleanroom

After an overnight purge test, material was found on a substrate. In this test, the gas flow is left on ovenight passing through the hot system, with the source valves closed, through the nozzle to the susbtrate. Since the source valves are

closed during this test, the depsotion found on the substrate is typically caused by a cold spot within the system. It is believed that the cold spot in our system is from the new nozzle which has an unheated narrow tip.

To test this theory, a thermocouple was mounted to the end of the nozzle to measure the temperture during deposition. During depsotion, the temperature at the tip of the nozzle was found to be 70° to 80°C below the set point. The nozzle was removed and examined for deposited material, but none was observed. The new nozzle has been removed and replaced with the original nozzle that has a much shallow tip to reduce the heat loss.

While Angstrom was at UDC repairing the valve heater and reinstalling the repaired carrier line, they upgraded the software such that each zone of the carrier line will be able to have a separate set point. Originally, there was only one set point for the 4 zones of the carrier line. This will allow us to "tune" the temperature of the carrier line to make it more uniform.

As system was being tested, there was an issue with trying to achieve deposition. After further investigation, it was found that the fittings for the valves inside two of the ovens were leaking. Rather than just tightening the fittings, all the ovens were shipped back to Angstrom Engineering to determine what was causing the fitting to loosen and leak since this has been an on going problem. While the ovens were at their facility, Angstrom was replaced all the valves heaters with heavier duty heaters to reduce the risk of the heaters shorting and failing.

While testing the ovens, Angstrom determined that the three valves (inlet, outlet and bypass) that were hard mounted to a plate on the back of the oven were preventing the tubing from expanding and contracting through temperature cycling. This caused excess stress on the fittings and when the fittings were released the tubing failed to line up. This problem has been fixed by allowing the two outside valves (inlet and outlet) to float, such that they can move with the expansions of the tubing as the oven heats up. Angstrom was confident that by lubricating the fittings and allowing the valves to float, the leak issues will be resolved, which is the case.

There has was an on going problem of over night deposition. This was occurring after a deposition was complete and the system purged after the deposition. The test for overnight deposition consists of a small flow of gas through the carrier line being left on over night with the nozzle parked over the substrate and then looking for deposited material on the substrate. With all the temperatures at least 50C above the host deposition temperature, there was no observable reason for any overnight deposition. After depositing material a system purging process to clean the organic material from all the carrier lines was developed. This process was based on a process that Michigan has developed to clean the dopant materials from the carrier lines in their system. The process combined a series of high flow purges alternating through both the nozzle and bypass valve followed by a pumping the system down to base pressure. Initially, after running the purging process, there was a small amount of overnight deposition observed

that was only visible under UV light. By optimizing the purging times the overnight deposition was eliminated.

Trials were run using several different purge times in an effort to reduce the total purge process. It was found that the limit of the purge time for each step was 2 minutes. The vacuum step was kept at 4 minutes as it take approximately 2 minutes to pump the system down to base pressure after purging the system, and ideally the system should be at base pressure for a period of time to allow any residue deposited material to evaporate. See Figure 29 for a flow chart of the process. Since the system requires several buttons for each step, Angstrom Engineering wrote a program to automate the process. The program was written to allow the user to select the N_2 flows, the purge times, pumping times and the amount of times the process can be repeated.

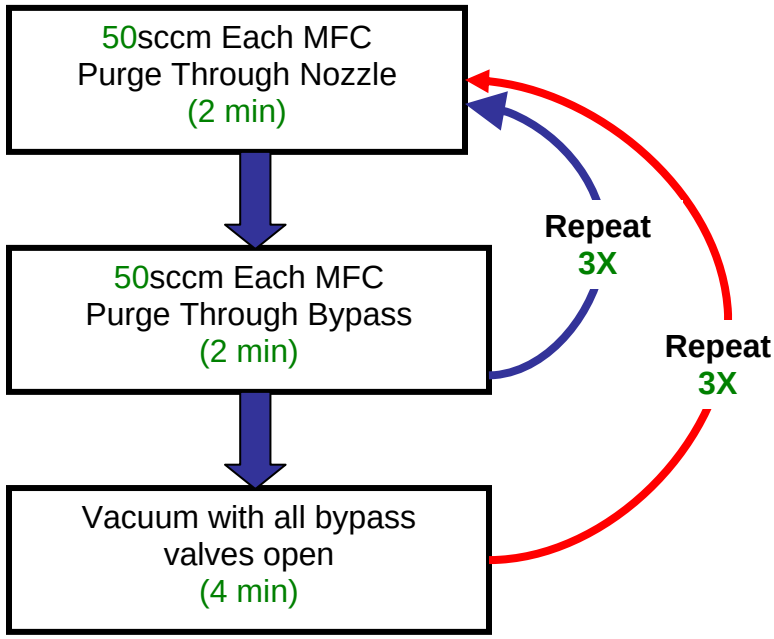

Figure 29: The above is a flow chart of the purge process that has successfully eliminated the overnight deposition. The parameters written in green will be user selectable.

In January 2008, the first OLED device was completed on the UDC OVJP system. See Figure 30 for the OLED device. The structure that was used was UDC's standard structure for a green device with the exception of the emission layer of CBP/Ir(ppy)$_3$ which was deposited by OVJP. Since a continuous OVJP deposition was used for each row of 3 test devices, the cathode metal was deposited on top of the OVJP deposited layer and did not make a good contact with the ITO cathode electrode. Although the device turned on,

Figure 30: First OLED device with a OVJP deposited emission layer made at UDC

direct contact to the cathode metal was required, thus the device will not be operational when encapsulated. A new metal shadow mask will be required with the opening in an L shape to ensure good cathode contact. See figure 31.

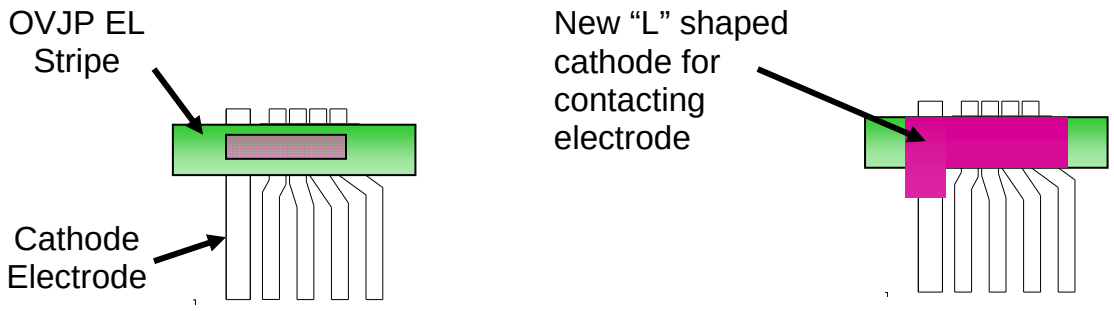

Figure 31: In the left diagram, the OVJP deposited EL (green) prevents cathode (purple) from contacting electrode as shown. In the right diagram, the new "L" shaped shadow mask makes good contact between the cathode and electrode.

J. Task 6.0 – Increased OVJP Printing Speed

Organic vapor jet printing using an array of parallel nozzles was successfully demonstrated. A multi-nozzle OVJP system was shown to be capable of both pattern generation and of growing high quality films of OLED applications. A successful multi-nozzle deposition system is an important milestone on the path from single nozzle OVJP experiments to an industrially useful OVJP process.

Nozzle arrays were fabricated from 1.53 mm OD stainless steel capillaries with a wall thickness of 130 µm. The nozzle array itself consisted of a row of five 130 µm holes drilled into the capillary by micro-electric discharge machining. The lengthwise direction of the row is parallel to the tube axis. The nozzle array was attached to the OVJP runline so that the nozzles face the substrate. A ceramic splint attached to the capillary by loops of 130 µm diameter stainless steel wire to increase rigidity. The wire also acted as a spacer to maintain a constant separation between the nozzles and substrate. (Figure 32) The nozzle array was resistively heated by passing DC current through the capillary itself.

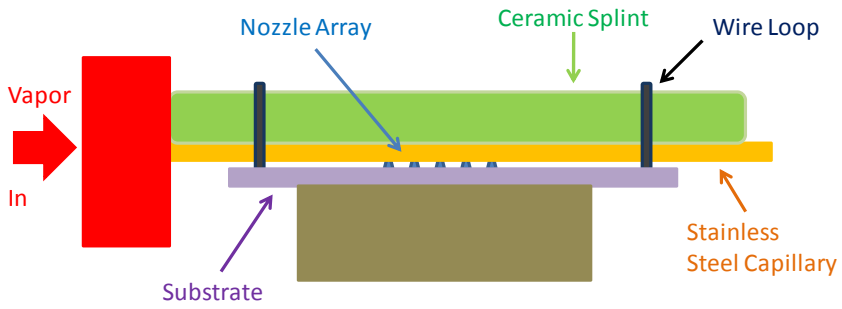

Figure 32: Schematic of nozzle array setup inside OVJP deposition chamber.

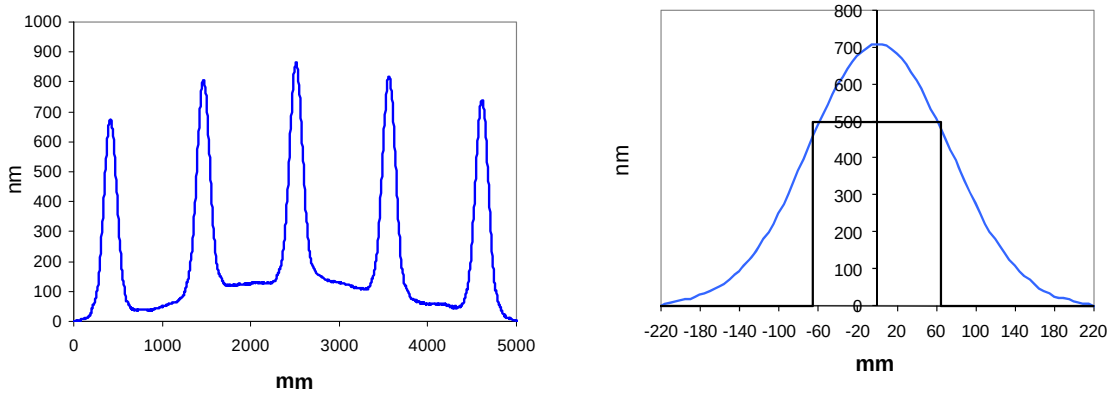

Figure 33: (left) A profilometric scan along a line perpendicular to the direction of the five lines printed by the nozzle array. The scan indicates a series of clean peaks, with the slow variation in baseline being an artifact of the instrument. (right) Closeup of one of the peaks. An ideal, flat deposition profile of width equal to nozzle diameter is shown in black for comparison.

Lines of CBP were characterized using profilometry. (Figure 33) Full width at half maximum for lines is 170 μm, which compares favorably with the nozzle diameter. Lines doped with $Ir(ppy)_3$ phosphoresced under a UV lamp. Visual inspection showed that the lines were sharp and no phosphorescence was visible between lines. (Figure 34)

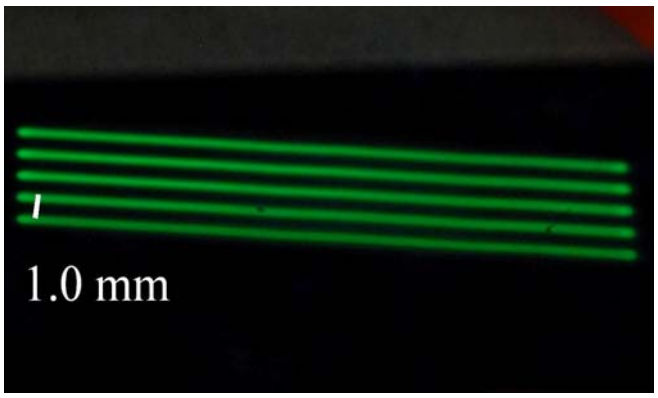

Figure 34: Lines of $Ir(ppy)_3$ and CBP drawn using a multiple nozzle array

In addition to drawing lines, the nozzle arrays can be used to evenly coat an area of substrate with organic material. The array was used in this mode to deposit the emissive layer of a $Ir(ppy)_3$/CBP green phosphorescent OLEDs. The device had efficiency comparable to similar VTE grown devices, with a peak forward facing power efficiency of 17.5 ± 4.0 lm/W and an EQE 7.0 ± 0.9 %. (Figure 35)

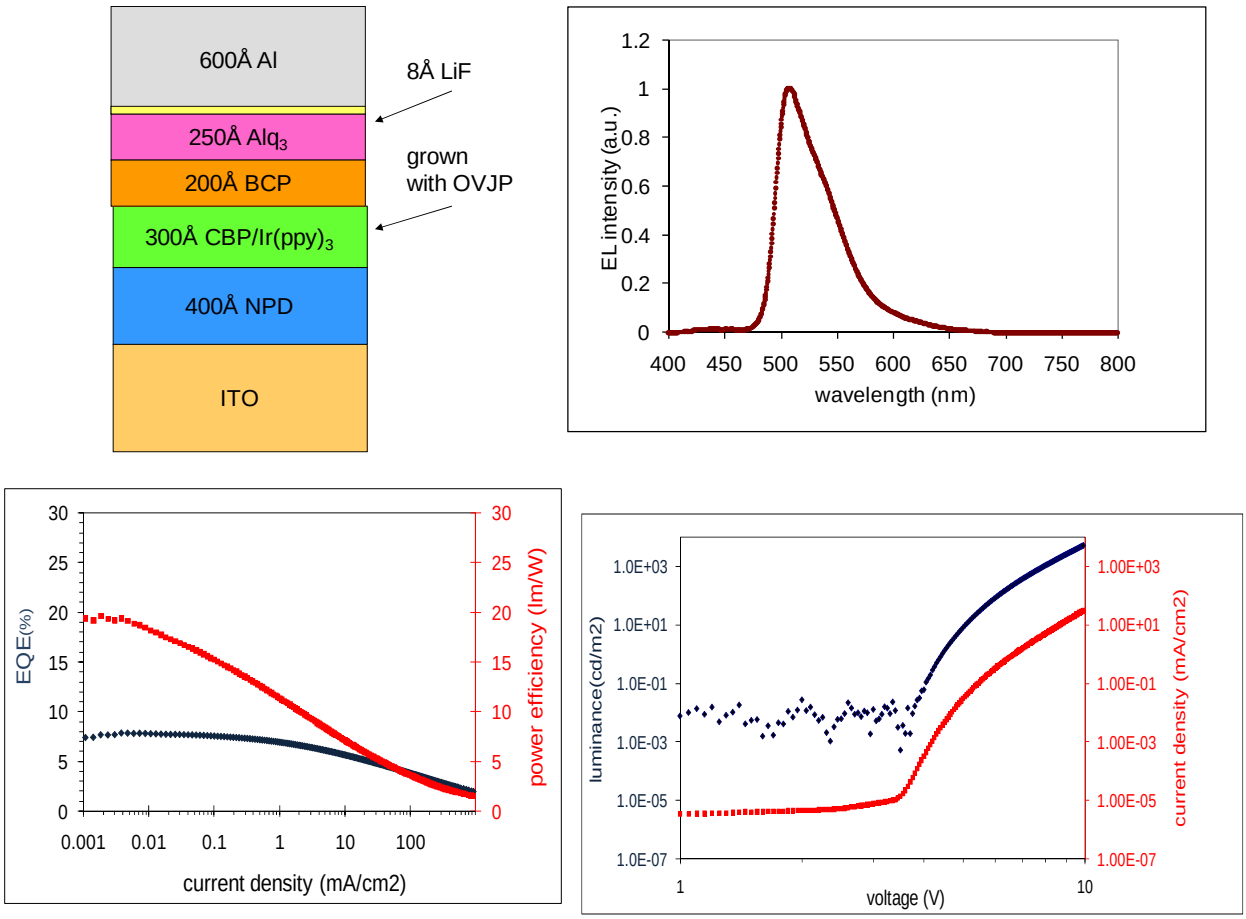

Figure 35: Phosphorescent OLED grown using OVJP parallel nozzle array. (upper left) The structure of the device. The emissive layer was grown using OVJP. Other layers were deposited in a vacuum thermal evaporator. (upper right) Electrophosphorescence spectrum generated by OLED. (lower left) External quantum efficiency and power efficiency curves generated by an OVJP processed device. (lower right) Current vs. voltage and luminance vs. voltage characteristics of a sample device.

PQIr doped CBP was also deposited. Different dopants can be used sequentially without contamination from the previous dopant. Dopant changes in OVJP previously required a lengthy purge cycle. A careful rearrangement of the backline appears have greatly reduced clearing time. Mixed patterns of PQIr and CBP stripes have been grown.

The OVJP system is in the process of being upgraded to enhance its capabilities and make it simpler to use. A rigid nozzle holder was machined and is being affixed to the inside of the chamber to provide the tighter tolerances required to achieve 30 μm features. Motor controllers and drivers for the motion stage are being replaced with a more powerful system to improve reproducibility. Finally, temperature will be controlled from by single computer interface, rather than from multiple independent thermostats, as is currently the case.

Following a successful demonstration of printing with an array of 130μm nozzles, printing with an array of 30μm nozzles was attempted. The 30μm nozzles were of similar construction to the previously used 130 μm nozzle array. Ten nozzles were etched into the wall of a stainless steel capillary in a row parallel to the axis. The nozzles were spaced 1mm center to center. The capillary containing the nozzles was connected to the terminus of the OVJP's runline and heated to 350ºC by passing 6 to 8A of direct current through it. A brace to rigidly hold the nozzle relative to the chamber was installed to improve patterning tolerances. See Figure 36. Previously, the capillary floated above the substrate on thin wire bearings.

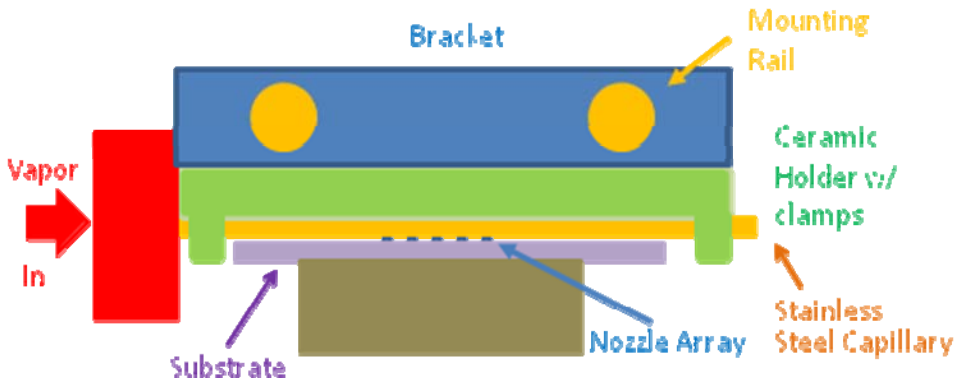

Figure 36: Experimental setup for nozzle array.

Initial attempts to deposit material using the new nozzle array and brace were unsuccessful. Minor problems such as leaks, kinks, and temperature irregularities were identified and repaired. However, deposition remained sporadic. The combination of small nozzles and a long runline may generate a prohibitive degree of stagnation in the OVJP system. The OVJP has a volume of approximately 300ml between the nozzle and organic sources. This would give vapor in the tube a residence time of roughly 13 minutes if the carrier gas feed rate is 2 sccm, typical for the 30µm nozzle array. This compares to a residence time of approximately 1 min for the 130µm nozzle array at a feed rate of 5 sccm. The runline was shortened as much as possible to allow for demonstration of the 30µm nozzle. Deposition can now be more readily observed. A redesign of the OVJP sources and runline to minimize internal volume while preserving multicolor doping capability may be desirable.

Lines of CBP with widths of roughly 100µm were obtained. (Figures 37 & 38) Based on experience with the 130 µm nozzles, it was expected that the smaller nozzles would be capable of producing features of 40µm or less. A misalignment between the stage and the cantilever which moves it, made it impossible to move samples close enough to the nozzles to achieve higher resolution.

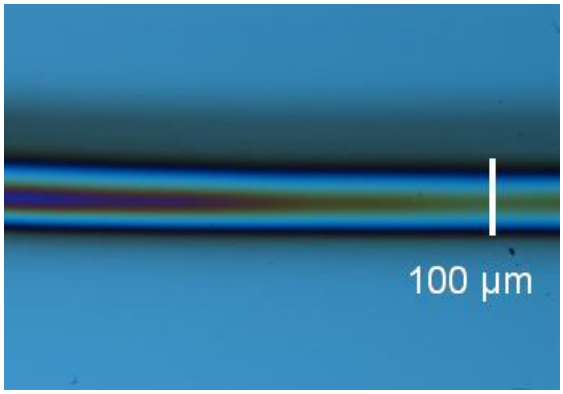

Figure 37: Micrographs of one of the lines drawn by the 30µm nozzle array.

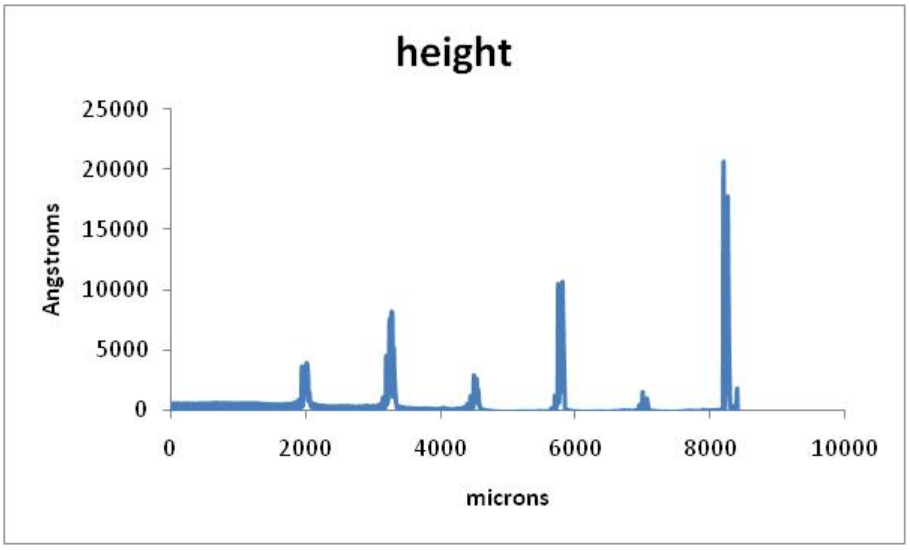

Figure 38: Thickness profile for a series of lines drawn using the 30µm nozzle array.

To realize an OVJP tool capable of printing multicolor device with high fill factor, it is necessary to improve upon the feature sizes and tolerances attainable with the current system. Previously, lines of approximately 100 µm in width were drawn using a 30 diameter µm nozzle. Attempts to further reduce feature size have not been immediately successful. The OVJP tool is being analyzed in detail to determine how to best meet these demanding specifications.

Preliminary modeling, combined with previous experience and the work in high resolution OVJP by Shtein et. al.[iv], suggest that a nozzle to substrate separation of approximately 5µm will be necessary to pattern segments of organic material that are 30 µm wide with 5µm separation between segments of different colors. This is the level of definition required for use with commercially available display backplanes. If segments of organic material are diffuse, rather than sharply defined, materials for different color OLED segments may become mixed, reducing device quality. Measuring and maintaining a 5 µm separation is beyond the capability of the current OVJP system.

Sensing nozzle to substrate separation has proven challenging. Contact sensors have already been tested and have been shown to tear organic films. Non-contact sensors must be compatible with nonmetallic substrates. Laser triangulation appears to be the most feasible distance sensing method. The sensor will have to be vacuum compatible as well as compact enough to mount on an OVJP print head. Commercially available laser triangulation sensors are being investigated for this application.

An improved stage will be necessary to achieve tight feature tolerances. A bend in the sample holder was corrected, and the height of the installed stage was measured in situ. A slope of 50µm per centimeter of long axis stage travel remained. It was determined that the cantilever which currently holds the stage does not provide adequate support. It will have to be supplemented by members inside the chamber. A linear piezoelectric actuator will be required to work in concert with the height sensor to provide fine height adjustment. The stage support and fine height adjustment are both under study.

Finally, the tolerances of the nozzle array itself will have to be improved to meet the 5µm specification. The previous steel capillary design tended to expand and arch when heated. Photolithographic processing of SiO_2 is being investigated as a way to produce an array of nozzles on a substrate that is both optically flat and relatively insensitive to thermal expansion. Many approaches to fabricating nozzles and connecting them to material sources have been developed for the field of microfluidics. A new print head design that will incorporate some of these techniques needs to be developed.

K. Task 7.0 – Demonstration of OVJP prototypes fabricated at UDC

A new substrate design was made specifically for the deliverable. See Figure 39. The lines are approximately 100mm long, 1mm wide and at a pitch of 1.5 mm. There are a total of 84 lines, which are 28 lines each of RGB.

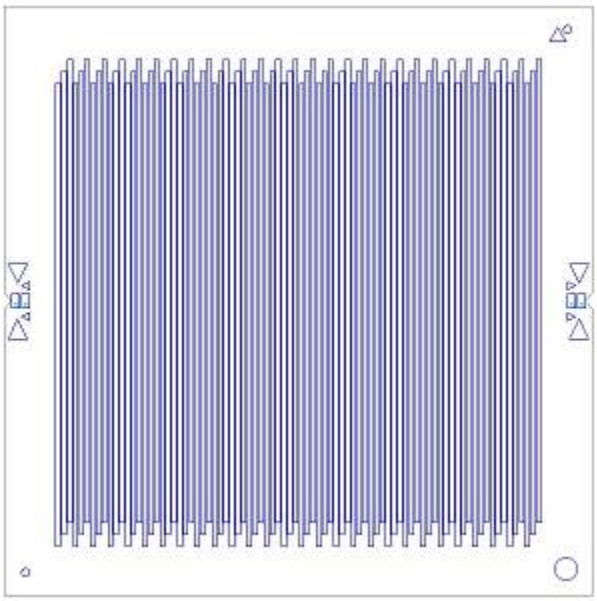

Figure 39: The design of the substrate for the deliverable. There are a total of 84-1 mm wide lines on a pitch of 1.5mm.

When we set out to calibrate the printed film thickness as a function of source vapor flow rate, the key variables that are monitored are: source temperature, flow rate through the source mass flow controller (MFC), stage translation speed and nozzle height.

The initial experiment drew lines on a Si calibration wafer, with the line thickness measured using single wavelength (633 nm) ellipsometry. A two-component source flow was used consisting of the host material plus green dopant. Source temperature, flow rates and nozzle height were kept constant and lines drawn at various stage speeds. See

Figure 40. The experiment was repeated twice on different days to ensure repeatability and the results are shown in Figure 41. The film thickness is, as expected, linear with reciprocal stage speed. The y-offset (51 – 79 Å) is attributed to the native oxide layer on the Si calibration wafers, which was not removed. There is, however, significant variation in the measured film thickness from run-to-run, which is of a magnitude that would make it impossible to reliably deposit high efficiency OLED structures (since optimal efficiency and device lifetime are sensitive to charge balance in the recombination zone and therefore film thickness). The printing rate appears to vary between 418 Å.mm/s and 608 Å.mm/s. We therefore turned our attention to the principal uncontrolled variable in the experiment, which were the system startup conditions.

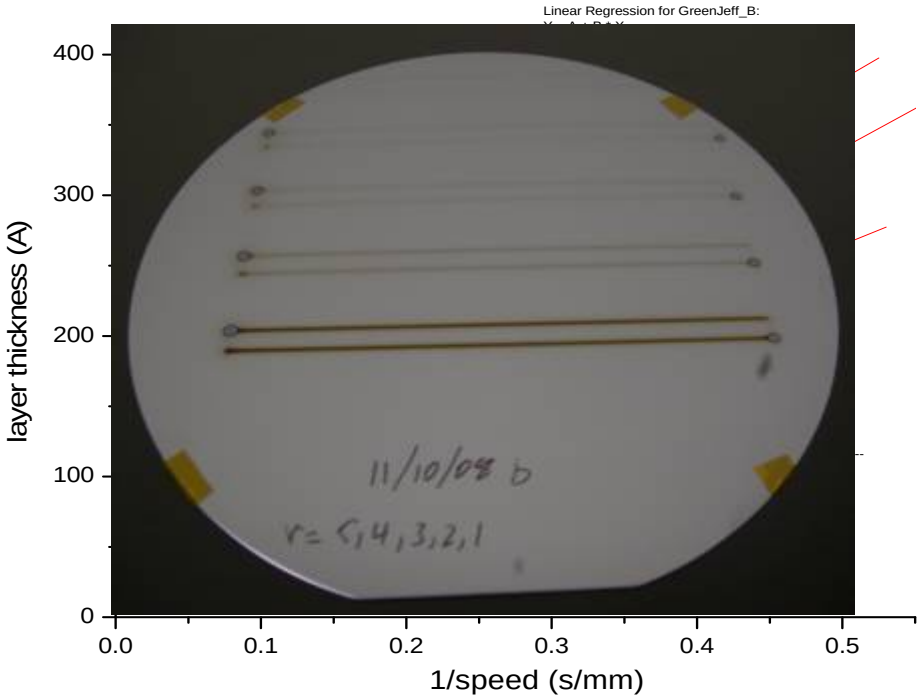

Figure 41 Figure 40: Wafer with deposition lines consisting of the host and green dopant materials deposited at stage speeds of 1, 2, 3, 4, and 5 mm/sec.

To achieve good color purity of the individual OLED elements, the deposition line must be thoroughly purged before starting to print. The startup procedure is to establish a flow through the source bypass line, then close the source bypass valve and open the source inlet valve to commence flow through the source. The deposition lag time is the time taken for the organic-bearing source gas to traverse the distance from the source to the nozzle. This is expected to be a function of the tube conductance and the source flow rate. A printing run starting from an empty nozzle is likely to result in a different film thickness than a printing run starting from a nozzle already filled with organic vapor. A

repeatable start up procedure was developed and it was used to calibrate the flows and thicknesses of each material.

Once the materials were all calibrated the first striped substrate was completed. For this substrate, the HIL, HTL, blue emitter and blue blocking layer were deposited in the VTE system before the red and green OVJP process. The green material was deposited first by OVJP, then the system was purged using a process of alternating high flows and evacuations of the chamber and carrier lines. The red material was then deposited by the OVJP. Once the red deposition was complete, the substrate was moved back to the VTE for the remaining layers.

When the device was turned on the red stripes were very dim and very green in color. The green stripes were also dim. We believe this is due to the "over spray" from the OVJP deposition of one stripe to the other. See Figure 42. To determine the distance of the over spray, a series of experiments were run by processing multiple lines of green next to multiple lines of red at different flows and stage speeds.

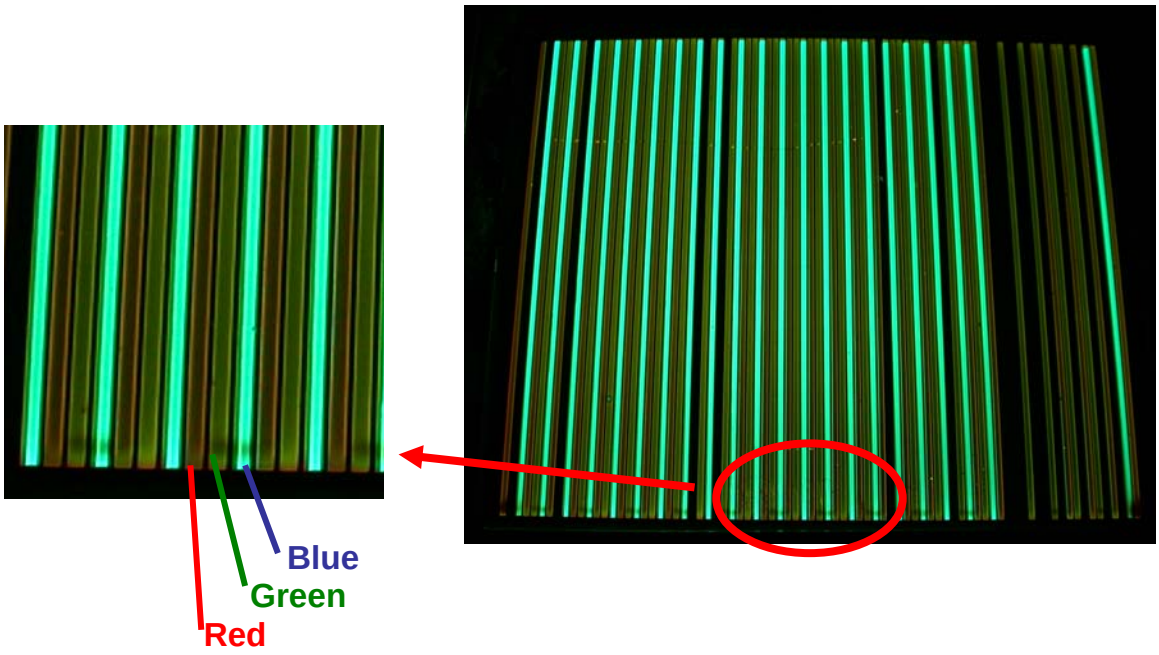

The first experiment run was to deposit 18 lines of green material followed by 18 lines of red material. When the device was turned on, it was found that the material being deposited by the OVJP nozzle has travel all across the substrate. See Figure 43. The lines where there was no OVJP deposition were brighter than where deposition took place. Initially it was thought that this may be due to the flows being too high, so the flows were reduced by 4X, from 40sccm total flow to 10sccm. During the recalibrating of the stage speed for the reduced green flow, it was found that at the same deposition thickness the lower flow crated a narrower line.

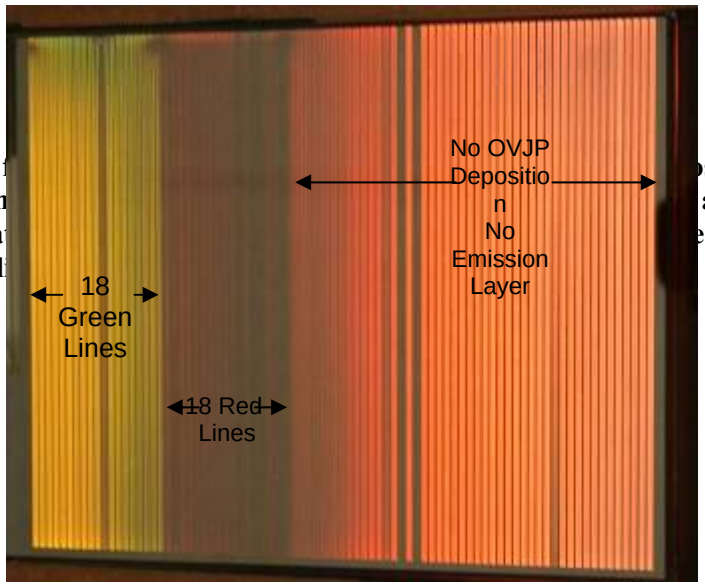

Figure 42: The f … osited by the OVJP system. The em … an "over spray" effect of the green ma… erial being deposited onto the green l… the camera.

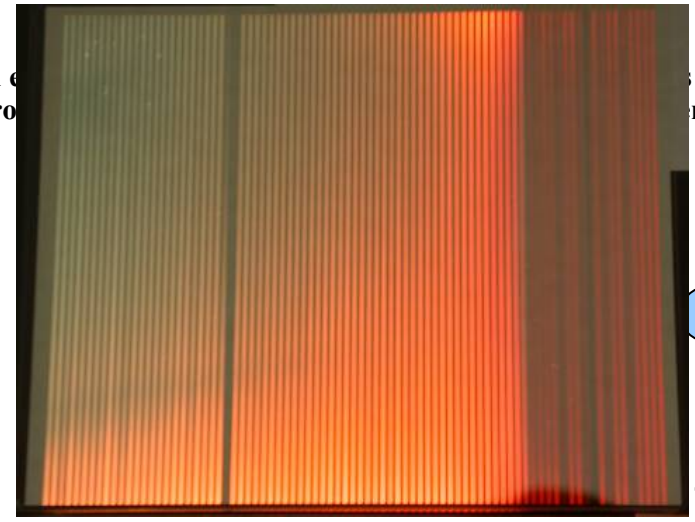

Figure 43: This is from an e… deposited followed by 18 ro… re was no OVJP deposition.

A substrate was process by depositing 18 rows of red material

at 4X lower flow (10sccm total flow). Although there was contamination beyond the 18 lines, it is not uniform over the entire substrate. After some investigation, it is apparent that some, if not all of the contamination is coming during the flow stabilization prior to deposition. The flows through the nozzle were run for 20 to 30 minutes before deposition to stabilize the flows through the nozzle. See Figure 44.

The next step was to further reduce the amount of material that could possibly come in contact with the substrate surface prior to the deposition process. During the flow stabilization through the nozzle, the time at the crystal monitor was greatly reduced along with keeping the nozzle tip below the plane of the front side of the substrate while at the home position. The combination of both reduced the over-spray on the substrate as seen in Figure 45. However, the over-spray on adjacent lines is still a problem due to different material being used for the adjacent RGB lines.

Figure 44: Striped substrate with reduced "over-spray" from the nozzle tip being below the plane of the substrate during flow stabilization

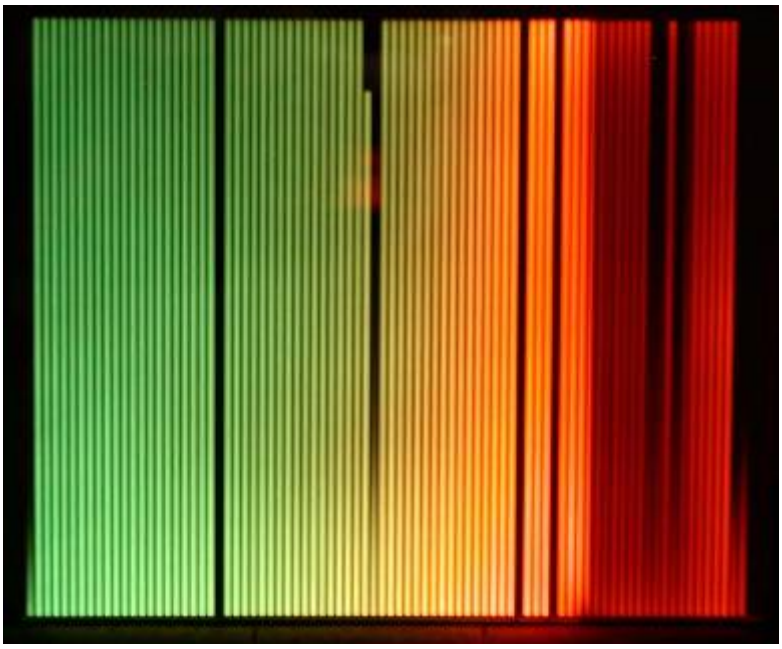

Figure 45: Red material deposited by OVJP on to the first 18 lines. The relative positions for the crystal monitor and home for the nozzle are marked. The nozzle is parked over the crystal monitor and home positions during flow stabilization. The over spray pattern is more evident on the side where the nozzle is parked.

To overcome the overspray on adjacent lines a new structure was selected in which a hole blocking layer was deposited on top of the EML right after the EML was deposited. The blocking layer for the blue and green are deposited through a shadow mask. See Figure 46 for the structure. The hole blocking layer was deposited by VTE. Although the blocking layers helped to reduce the impact of the cross contamination during the OVJP deposition process, the red emission was dim when a full color substrate was made. See Figure 47.

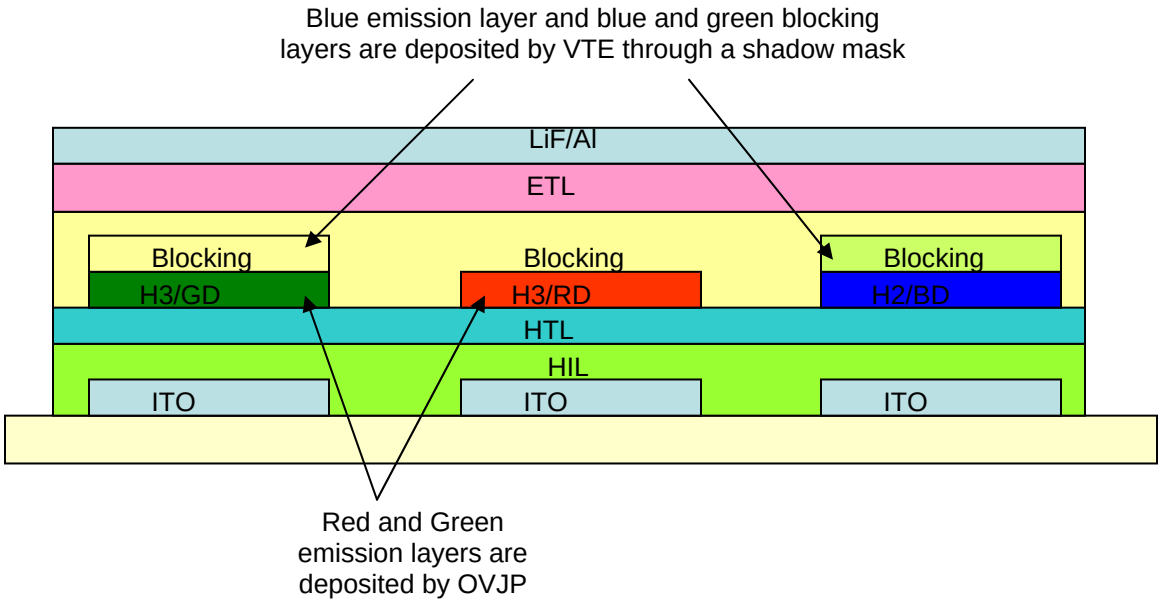

Figure 46: Layer Structure of the striped substrate. The blue blocking layer is deposited prior to the green OVJP deposition and the green blocking layer is deposited prior to the red OVJP deposition

To determine the cause of the poor red emission a series of testing was performed. First, a striped substrate was made with only the red material deposited on to it. Second, a striped substrate was made with the blue material deposited by VTE and then the

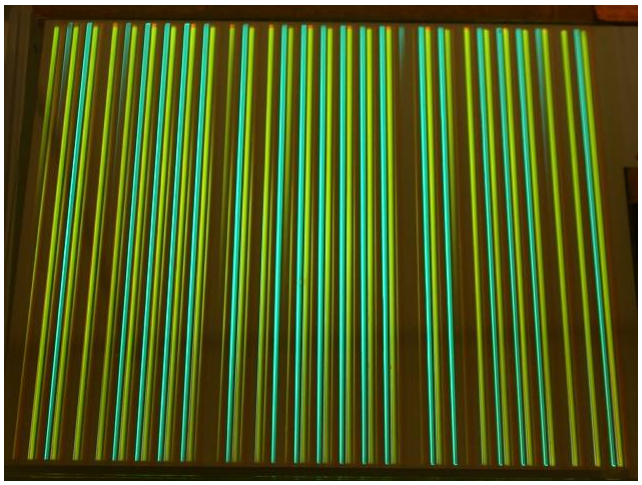

Figure 47: Full color substrate in which the red lines are very dim

red material deposited by OVJP. For the red only substrate, it was found that the lines adjacent to the OVJP deposited lines were more efficient than the OVJP deposited lines. The peak wave length for both the OVJP deposited line and the adjacent lines were the same. See Figure 48. It is believed that the lower brightness may be due to the deposited red material being over heated and degraded. The temperature of the nozzle is 350C and the distance between the nozzle and substrate is 1mm. Since the tip is only directly over the deposited line, the adjacent lines are not as affected. To reduce the effect of the hot nozzle, the travel speed of the substrate was increased by 2X and the material was deposited using 2 passes to get the desired thickness on the next substrates.

For the blue and red substrate, the brightness of the red emission was found to be less than 10% of the red only substrate. The peak wave length on both substrates was the same. The cause of the reduced emission is due to the blue blocking layer traveling under the shadow mask on to the red line. Further studies will be required to determine the best method to reduce the organic materials from traveling under the shadow masks. On other deposition systems, magnets are used to hold the shadows masks tightly against the substrates.

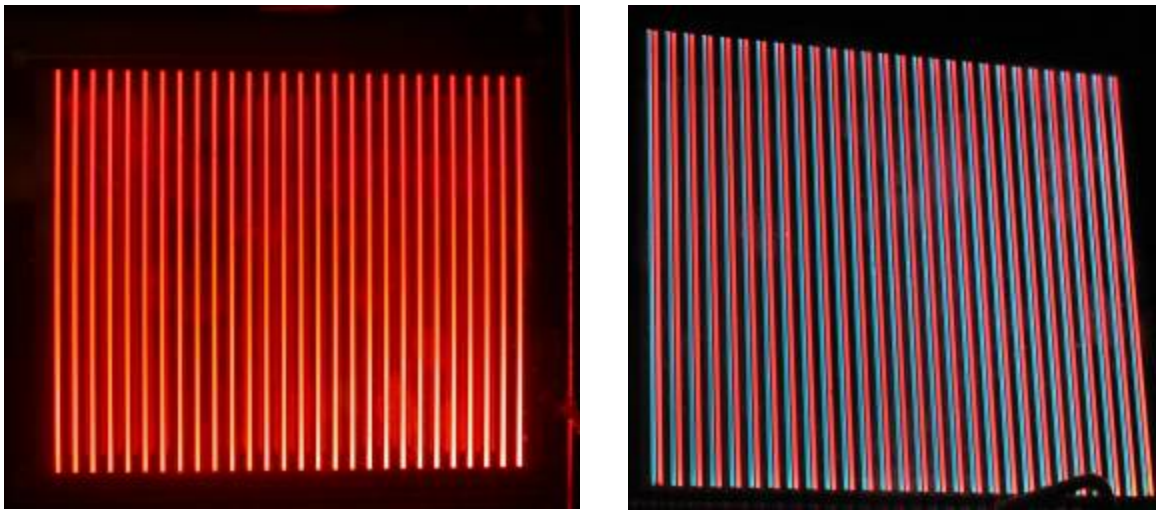

Red Lines	**Cd/m2**	**Peak**	**Voltage**	**CIE(x,y)**
Red Deposited Row Red Only Substrate	493	634	17.3	0.680,0.316
Adjacent Row Red Only Substrate	611	628	16.4	0.670,0.317
Red Deposited Row Red/Blue Substrate	33.9	634	20.2	0.680,0.315

Figure 48: Performance of deposited OVJP deposited red lines on a substrate with only the red deposited line (left) and with blue VTE deposited lines (right).

From all the experiments that were run, several process changes were made and a full color substrate was made. The process changes included: moving the nozzle to a location below the plane of the substrate during flow stabilization to reduce the random deposition on the substrate; reducing the process flow by 4X to reduce the "over-spray" an to adjacent rows; depositing a blocking layer on top of the blue lines before the green OVJP deposition and on top of the green lines before the red deposition to reduce the effect of the 'over-spray"; increase the travel speed of the substrate to reduce the heat transfer to the OVJP deposited lines. The result of the process modifications was a full color substrate as seen in Figure 49.

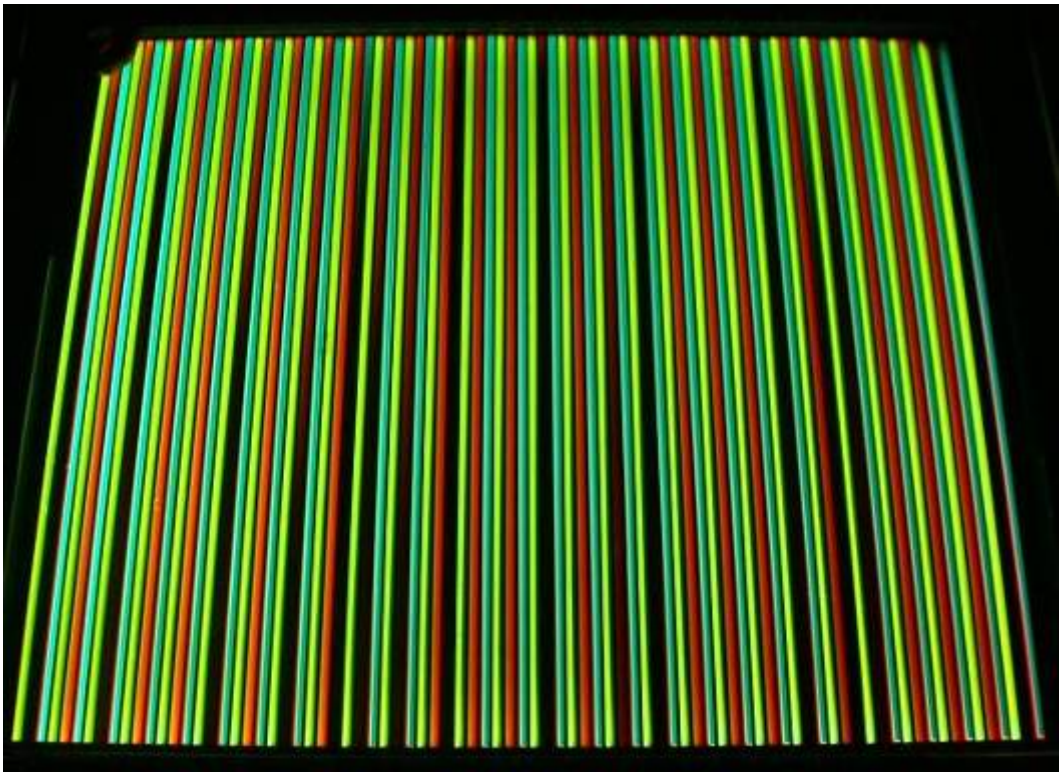

Figure 49: Full color striped substrate with red and green emission layers deposited by OVJP

Although the OVJP program has ended, the work on OVJP is continuing. We will be continuing to work on reducing and eliminating the "over-spray" problem. We will be investigating and modeling to determine the extent of the problem. Initial key area that will be investigated is chamber pressure and substrate temperature. We expect that both of these have a big influence as to the distance the material travels across the substrate. Also, we will be continuing to investigate the size of the deposition footprint. Smaller size nozzles and multiple nozzles will be designed and tested to determine the minimum size deposition that is achievable. This work will be based on and will be a continuation of the work that the University of Michigan has performed in this program.

To continue the work on the OVJP, the tool will need to be modified to overcome some of the current design limitations. The flow that is currently used during the depositions is just above the bottom limits of the mass flow controllers (MFC). Lower range MFCs will need to be installed to improve the repeatability of the flows along with one high range MFC that will be used for system purging after a process. The movement of the stage is very limited. The stage movement program is currently independent of the process flow operation. Programming changes will need to be installed such that flows can be turned on and off at certain stage locations. In the current system, the time it takes the material to reach the nozzle is from when the flow is turned on is long. This lag time needs to be reduced, which may require reconfiguring the furnaces to be closer to the nozzle. Further modeling and experimentation will be required to determine the best design. Once these design limitations are completed, it is expected that improved results will be achieved.

L. Task 8.0 – Commercialization Roadmap

Given the tremendous amount of energy consumed by both commercial and residential lighting (approximately 7 quads, or over 1 billion barrels of oil equivalent in the US alone), it is critical that we develop new environmentally friendly, aesthetically pleasing and energy efficient forms of lighting. Over the last few years there has been very significant progress in the development of solid state lighting. This started through inorganic LEDs attaining very high efficacies (now up to approximately 150 lm/W) for small high luminance light sources, and now with organic LEDs (OLEDs), which have recently achieved efficacies of over 100 lm/W. These technologies are complementary, with LEDs providing high intensity point source lighting, and OLEDs providing an energy efficient, large area, and very pleasing form of environmentally friendly solid state lighting

Using UDC's phosphorescent OLED (PHOLED™) technology, efficacies in excess of 100 lm/W have now been achieved. Moreover, because of their large area form factor, and low voltage drive requirements, there are few system losses from either power supplies or diffusing optics (as compared to all other forms of lighting). This allows an OLED luminaire efficacy to be extremely competitive with the best fluorescent or LED fixtures. OLEDs are appealing sources of light, because they are thin and light weight devices, which can also be formed on conformable or flexible substrates, and be available in all shapes and sizes. Their warm white color is ideally suited for indoor illumination applications. One differentiating factor from conventional light sources, is that using OLEDs one has the ability to produce color tunable lamps, which is very attractive for a number of consumer applications. This is enabled by producing individual red, green and blue OLEDs on the same substrate, and individually addressing the three primary colors.

From our discussions with several leading U.S. lighting integrators, there is a great desire to manufacture OLED based solid state lighting. For this to happen there needs to be a source of OLED lighting panels. Our goal through this work, has been to develop the OVJP technology, and then transfer and license it to OLED manufacturers, who will then provide lighting panels for U.S. lighting integrators to make into OLED luminaires.

As shown by the technical work performed under this program, we believe that OVJP is a very promising technology to produce low cost, high efficacy, color tunable light sources. While we have made significant progress to develop OVJP technology and build a pilot line tool to study basic aspects of the technology and demonstrate a lighting panel prototype, further work needs to be performed before its full potential and commercial viability can be fully assessed.

In particular we recommend further studies be performed related to:

- Detailed analysis of source utilization
- Further characterization of the relationship between printing speed, material flow rates, and printing resolution.
- Transfer of the OVJP process to prototype manufacturing equipment (e.g. Gen 2 substrate size) with appropriate system performance metrics

Given the recent rapid progress in the efficacy of white OLEDs, and the accompanying improvement in their lifetimes, another key challenge for the adoption of OLED lighting is cost reduction. While the cost of an OLED panel is determined by several factors, we need to ensure that the OLED deposition process is at least 60% efficient.

In fact, assuming 110 lm/W OLED lighting by 2015, and a price point around $10 per klumen, we can expect OLED lighting to save 0.55 quads of electricity, or close to 10% of the current total U.S. electricity use for lighting, representing an annual savings equivalent to almost 100 million barrels of oil. This work will lead to lower lamp costs, as for OLED lighting to achieve the critical milestone of less than $10 per kilolumen, it is necessary that OLED deposition processes be established with at least 60% of the organic materials being utilized in the final product.

Although this DOE funded program to develop OVJP has now ended, UDC is committed to developing technologies to enable cost effective, high efficacy WOLED lighting. This involves further development of our phosphorescent OLED technology, in addition to key manufacturing technologies. We see OVJP as such a key manufacturing technology. UDC is therefore planning to continue technical progress of this work under its own funding, addressing the outstanding technical issues, listed above.

In addition, we intend to partner with one or two leading OLED manufacturers, to transfer our technology to them, to assess its viability for large area manufacturing of OLED devices. If this is successful, we intend to license the technology, and work closely with these manufacturing partners to enable the production of OLED lighting panels.

Once we have established a panel manufacturing capability using OVJP, we will work closely with U.S. lighting integrators to develop OLED lighting products. This will then provide the U.S. with a competitive OLED based solid state lighting industry with OLED luminaires being manufactured in the U.S.